CHAPTER 13

Screening for Reactive Metabolites Using Genotoxicity Arrays and Enzyme/DNA Biocolloids

JAMES F. RUSLING, ELI G. HVASTKOVS, and JOHN B. SCHENKMAN

13.1 INTRODUCTION

Therapeutic drugs and chemicals used in our bodies or in our environment must be guaranteed safe to the people who are exposed to them. Extensive procedures for screening and predicting toxicity have been developed in the pharmaceutical industry. Nevertheless, drugs that are toxic to some subset of the population are not always identified by these procedures. About 30% of drug development failures are linked to toxicity issues, and unfortunately some of these do not come to light until clinical trials or even after the drug is introduced to the market. In addition, drug costs correlate with drug development failures (Caldwell and Yan, 2006). For these reasons, predicting drug toxicity at the earliest stages of development has become a critical goal (Nasser, Kamel and Clarimont, 2004).

A wide variety of strategies have been proposed for early toxicity prediction, including *in silico* methods along with a range of *in vitro* and *in vivo* biological approaches (Nasser, Kamel and Clarimont, 2004; Mayne, Ku and Kennedy, 2006; Kramer, Sagartz and Morris, 2007). Established methods use microsomes, cell cultures, or animal models and tend toward utilization of biochemical end points that are the result of complex responses to the drug (Kramer, Sagartz and Morris, 2007). These methods are typically combined into a panel of methodologies that in many cases provide a reasonably good prediction of human *in vivo* toxicity (Mayne, Ku and Kennedy, 2006). Nonetheless, unpredicted or idiosyncratic drug toxicity can result from interindividual variations in human biochemistry and resulting drug behavior in specific individuals that may be impossible to predict from batteries of toxicity tests and sometimes even from human clinical trials limited to subsets of the population that will eventually use the drug.

Certainly existing toxicity testing and prediction methods are important, viable, and useful. However, there is an unfilled niche for simple, cheap, high-throughput,

Drug Metabolism Handbook: Concepts and Applications, edited by Paul F. Hollenberg, JoAnn Scatina and Ala F. Nassar

biochemically based screening assays that can be arranged into biosensor or biosensor array formats that are currently emerging (Stoll *et al.*, 2004; Rusling, Hvastkovs and Schenkman, 2007). Inexpensive toxicity devices of this sort could be used at very early stages of drug development and contribute important information about toxic drug candidates to aid in screening decisions. While the development of such sensing devices is in its infancy, this approach has the potential to help decrease drug development expenditures and, ultimately, costs of drugs to the public. In this chapter, we discuss fabrication and measurement principles for such devices, as well as recent examples of such approaches.

Reactions of DNA with drug molecules or their enzyme-generated metabolites can produce covalently linked nucleobase adducts which may initiate cancer (Jacoby, 1980; Friedberg, 2003; Scharer, 2003). These adducts most often occur on guanines and adenines in DNA, and serve as good biomarkers for cancer risk (Warren and Shields, 1997; Phillips *et al.*, 2000). They are also convenient biomarkers for detecting reactive metabolites and predicting drug toxicity (Tarun and Rusling, 2005a; Rusling, Hvastkovs and Schenkman, 2007). The reactive metabolites also modify proteins and other biomolecules, but DNA adducts are readily measured by a number of modern bioanalytical techniques including liquid chromatography–mass spectrometry (LC-MS). "Bioactivation" is the term used to denote generation of reactive metabolites by cytochrome P450s (cyt P450) and other metabolic enzymes. The process of forming of reactive metabolites and causing DNA damage is usually called genotoxicity. Many substrates yield DNA-reactive metabolites, including styrene, benzo[*a*]pyrene (B[*a*]P), nitrosamines, napthylamines, and tamoxifen and other chemotherapeutic agents (Bond, 1989; Cavalieri *et al.*, 1990; Pauwels *et al.*, 1996; Umemoto *et al.*, 2001; Wang *et al.*, 2001). These reactive intermediates can also damage proteins and other biomolecules. In general, there is much more published information about the chemistry of reactive intermediates from nondrug molecules such as pollutants, since information for drug candidates that never came to market may be considered proprietary.

Cyt P450s are metabolic iron-heme enzymes (P—Fe) that catalyze the transfer of oxygen atoms to organic substrates (Schenkman *et al.*, 1993; Lippard and Berg, 1994; Ortiz de Montellano, 2005). Figure 13.1 depicts an accepted mechanistic model for cyt P450 enzyme catalysis that can lead to bioactivation. The resting state of the catalytic iron heme has water bound to the distal side of P—Fe(III) **(1).** This water freely exchanges with its environment and does not participate in oxygen transfer reactions (Lippard and Berg, 1994). This form of the enzyme binds the substrate RH and eliminates the distal water **(2).** Substrate is not bound directly to the iron heme of P—Fe(III), but sits above it in a hydrophobic pocket within the protein. Next, **2** is reduced by one electron to the P—Fe(II) state by an NADPH-dependent reductase to give **3**. P—Fe(II) **3** then binds dioxygen at the distal site to form a ferrous-dioxygen or ferric superoxy complex **(4)** (Guengerich, Bell and Okazaki, 1995; Guengerich, 2001; Ortiz de Montellano and De Voss, 2002). This P—Fe(II)—O_2 complex is converted to a P—Fe(III)—OOH complex via a one-electron reduction to give **5**, then protonated to **6**. The electron to generate **5** comes from an NADPH-dependent reductase in most cases. P—Fe(III)—OOH **(6)** may also be generated by addition of hydrogen peroxide or organic peroxides in a reversible process called the peroxide shunt. Protonation of **6** and dioxygen bond cleavage leads to formation of the highly reactive heme-iron(IV)-oxo radical cation {(P•+)Fe(IV)-oxo, **7**}, which transfers oxygen to the bound substrate to generate the product (ROH). The product dissociates from the enzyme and the distal site is reoccupied by water for another catalytic cycle. In addition, exposure of ferrous form **3** to

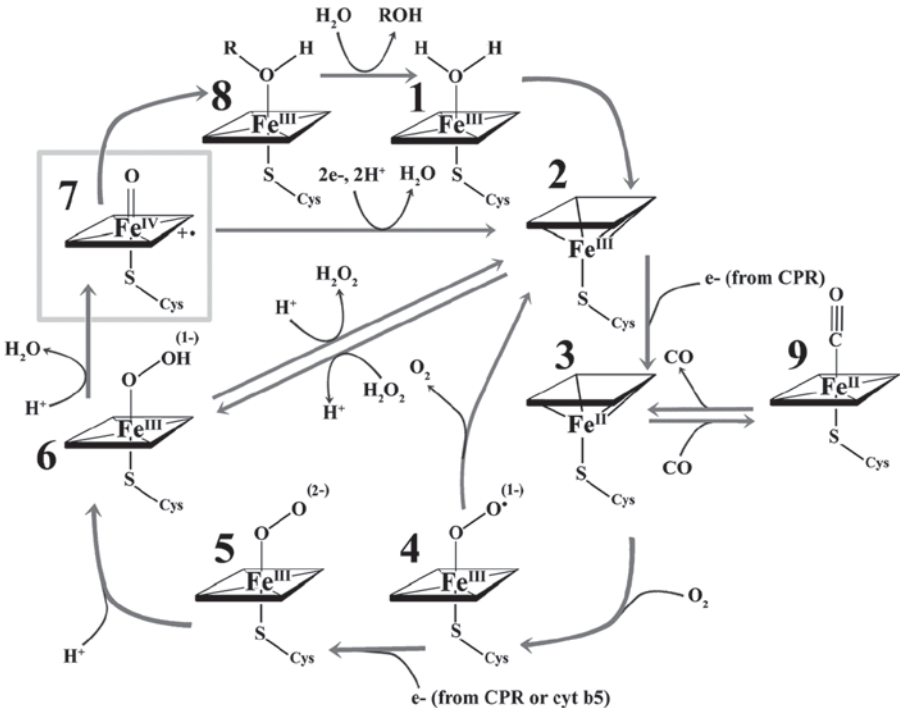

Figure 13.1 Pathway for cyt P450-catalyzed metabolic reactions.

carbon monoxide produces the P—Fe(II)—CO complex **9** that absorbs light at ~450 nm and gives cyt P450s their characteristic name.

A simple example of bioactivation involves the conversion of styrene to styrene oxide by cyt P450 enzymes. In this case, styrene oxide is the only enzyme-generated metabolite. We use this example to show how the natural bioactivation process can be mimicked to produce and detect.

DNA damage can be used as an end point for formation of the reactive metabolite styrene oxide. In Fig. 13.2, we see that if styrene is converted to styrene oxide by a cyt P450 enzyme in the presence of DNA, DNA will be damaged, mainly by forming covalent adducts with guanine bases (Tarun and Rusling, 2005a; Rusling, Hvastkovs and Schenkman, 2007). Further, we show how thin films of metabolic enzymes and DNA grown on arrays or colloidal particles can facilitate detection of these damage events, rapidly and nonspecifically by novel array technology, or more specifically by capillary LC-MS/MS.

In the next section, we describe how these concepts can be utilized to make electrochemiluminescent arrays for drug screening, specifically addressing formation of reactive intermediates, genotoxicity, and enzyme inhibition. In Section 13.3, we show how the same concepts can be used for the rapid, sensitive identification and quantitation of major reactive intermediates and their nucleobase adducts by capLC-MS. In Section 13.4, we survey alternative emerging technologies including optical protein microarrays that can be applied to drug toxicity screening.

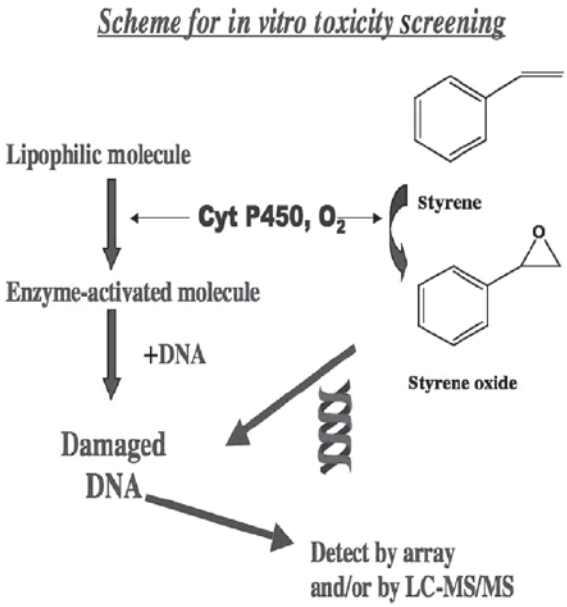

Figure 13.2 Illustration of scheme used for toxicity screening from the formation of reactive intermediates using DNA damage as a measured end point.

13.2 ELECTROCHEMICAL AND ELECTROCHEMILUMINESCENT ARRAYS

A major research effort in our laboratory has been directed toward developing biosensor arrays for genotoxicity screening (Rusling, 2004, 2005; Rusling *et al.*, 2007; Rusling, Hvastkovs and Schenkman, 2007). These arrays all utilize a versatile layer-by-layer film fabrication technique (Lvov, 2000, 2001; Ariga, Hill and Ji, 2007; Zhang, Chen and Zhang, 2007) to grow 20- to 40-nm-thick films containing metabolic enzymes and DNA (Fig. 13.3). These films facilitate the two-step process illustrated in Fig. 13.2. That is, the enzyme reaction produces metabolites that may or may not damage DNA, and the array measurement step detects the relative degree of DNA damage.

The enzyme reaction is the first step of array operation. It was established long ago that metabolic specificity is a property of the terminal oxidase, cyt P450 (Rahimtula *et al.*, 1978; Werringloer, Kawano, Estabrook, 1980; White, Sligar, Coon, 1980; Adams and Adams, 1992). Thus, cyt P450 enzymes in the films can be activated by small concentrations (≤1 mM) of hydrogen peroxide, in the reverse of the well-known hydrogen peroxide shunt (see Fig. 13.1), to give identical products as when the natural oxidoreductase system is used. A few reports documented cases of altered product distributions when cyt P450s were activated using peroxides as opposed to the natural electron donor/reductase cycle (Bichara *et al.*, 1996; Kupfer *et al.*, 2001; Ortiz de Montellano, 2005). However, in all cases examined in our laboratory, hydrogen peroxide activation gives the same metabolites as natural cyt P450 activation by NADPH and cyt P450 reductase. Thus, peroxide activation is appropriate and convenient for use in these sensors. In addition, we shall see that these arrays can also be made using liver micro-

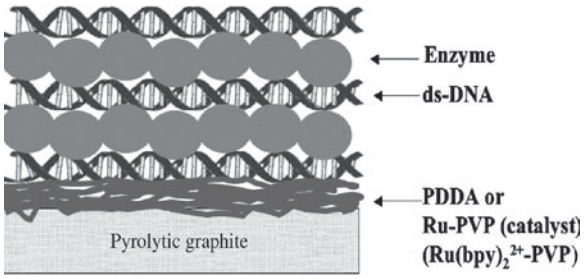

Figure 13.3 Idealized representation of enzyme/DNA films that can be made on any solid surface. The enzyme reaction produces metabolites in close proximity to DNA. In arrays, resulting damage to DNA from the metabolites is detected by voltammetry or electrochemiluminescence.

$$ClRu^{II}\text{-}PVP \leftrightarrow ClRu^{III}\text{-}PVP + e^{-} \text{ (at electrode)} \quad (13.1)$$

$$ClRu^{III}\text{-}PVP + G \rightarrow ClRu^{II}\text{-}PVP + G^{\bullet} + H^{+} \quad (13.2)$$

Scheme 13.1 Catalytic electrochemical pathway for detection of DNA damage using ClRu-PVP.

somes as the source of metabolic enzymes, and activated by NADPH and cyt P450 reductase as in living systems.

The enzymes in the "nanoreactor spots" on the arrays synthesize reactive metabolites near large concentrations of DNA in each film spot. The rate of DNA damage from metabolite–nucleobase adduct formation is a measure of relative genotoxicity, and can be detected by voltammetric (Wang *et al.*, 2005) or electrochemiluminescent (Hvastkovs *et al.*, 2007) measurement steps.

Arrays for genotoxicity screening arose from of our research on single electrode biosensors that established the optimized parameters and operating conditions (Rusling, 2004, 2005; Rusling, Hvastkovs and Schenkman, 2007). The enzyme reaction is the first step of sensor operation. We ascertained that pH ~5.5 was optimum for DNA damage (Rusling, 2004, 2005), and that enzyme/polyion films 20–40 nm thick eliminate performance limitations from mass transport of reactant entering the film and product leaving (Munge *et al.*, 2003). The second step in the assay is detection of DNA damage, and we found that electrochemical detection with very good S/N can be done with square wave voltammetry (SWV) for DNA oxidation using a soluble electrochemical catalyst, $Ru(bpy)_3^{2+}$ (Zhou *et al.*, 2003; Wang *et al.*, 2005). Alternatively, a catalytic Ru-polyvinylpyridine polymer [$Ru(bpy)_2^{2+}$Cl-PVP or ClRu-PVP) can be incorporated within the film for "reagentless" sensing (Mugweru, Yang and Rusling, 2004). The signal in the measurement step after the enzyme reaction results predominantly from catalytic electrochemical oxidation of guanines in DNA (Scheme 13.1). Here, the catalyst active sites have better access to guanines in the partly unfolded, damaged DNA than in intact ds-DNA. Improved access of catalyst to the guanines provides faster rates of the reaction (Eq. 13.2) in damaged DNA that in undamaged ds-DNA and consequently larger signals (Rusling, 2004, 2005; Rusling *et al.*, 2007).

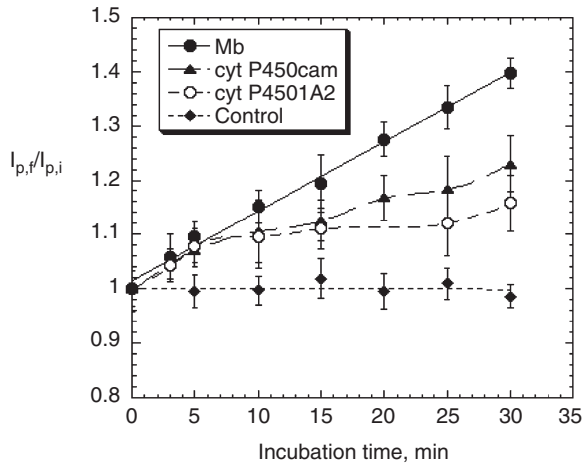

Figure 13.4 Influence of incubation time with 50-μM benzo[*a*]pyrene and 1-mM H_2O_2 on the final/initial peak current ratios from SWV of PDDA/DNA/(enzyme/DNA)$_2$ films in an eight-electrode array. Control is PDDA/DNA/(Mb/DNA)$_2$ film in 50-μM benzo[*a*]pyrene alone (four replicates for Mb films, three each for cyt P450 films). Amounts of proteins in the films in nmol cm^{-2} were 0.26 for Mb, 0.060 for cyt P450cam, and 0.054 for cyt P540 1A2. Adapted with permission from Wang *et al.* (2005). Copyright 2005 American Chemical Society.

Prototype genotoxicity screening sensors in the format described combined enzyme bioactivation leading to potential DNA damage, mimicking events in the human liver. Direct measurement of formation rates of altered nucleobases by LC-MS from similar films that had been reacted with damage agents and hydrolyzed confirmed that the sensors actually detect DNA damage (Tarun and Rusling, 2005a). Sensor and LC-MS results also correlated well with animal genotoxicity estimated by TDL_o, that is, the lowest dose producing carcinogenicity, in mice and rats (Tarun and Rusling, 2005a; Yang, Wang and Rusling, 2005).

Inclusion of several cyt P450s in electrochemical arrays facilitates analysis of the relative ability of the enzymes to generate genotoxic intermediates. Our first such array had eight electrodes and included cyt $P450_{cam}$, human cyt P450 1A2, and myoglobin (Mb) (Wang *et al.*, 2005). Mb is a good control in these arrays as it catalyzes some of the reactions of cyt P450s, but usually much less efficiently. In an array with cyt P450s, it should be the least active enzyme or have no activity at all. B[*a*]P was used as a test substrate for these arrays because of its well-understood metabolism resulting in several DNA-reactive metabolites from cyt P450-catalyzed oxidations (Rogan *et al.*, 1993; Todorovic *et al.*, 1997; Neilson, 1998). DNA damage was detected by increases in SWV peak ratios using soluble $Ru(bpy)_3^{2+}$ as the catalyst. Figure 13.4 shows the influence of enzyme incubation time on final/initial sensor peak ratio from such an array. Initial slopes of these plots divided by the amount of each enzyme in the array spots give relative turnover rates in {(nmol enzyme)$^{-1}$ min^{-1})}, which were of 3.0 for cyt $P450_{cam}$, 3.5 for cyt P450 1A2, and 0.9 for Mb. Cyt $P450_{cam}$ and cyt P450 1A2 showed threefold higher activity for bioactivation of B[*a*]P for DNA damage than the control enzyme Mb.

The ability to detect metabolite-based DNA damage simultaneously for several enzymes represents a promising approach to identify and characterize genotoxicity

pathways. However, the electrochemical arrays described require individual, electronically addressed electrodes and reproducible microelectronic chip manufacture. While this is certainly possible, an instrumentally more convenient approach is based on optical detection of electrochemiluminescence (ECL) from damaged DNA using a similar catalytic detection scheme. This approach requires no special electronics, and detection can been done with a simple charge-coupled device (CCD) camera.

Using ECL, application of a voltage to a polymer in a simple array can produce light. In the absence of DNA, when oxidation catalyst $Ru(bpy)_3^{2+}$ is oxidized to $Ru(bpy)_3^{3+}$, ECL has been generated by using a sacrificial reductant, often tripropylamine or oxalate. This produces a photoexcited $[Ru(bpy)_3^{2+}]^*$ by a pathway involving reaction of a radical form of the reductant with electrochemically generated $Ru(bpy)_3^{3+}$ (Ege, Becker and Bard, 1984; Kenten *et al.*, 1991; Xu *et al.*, 1994). Alternatively, $Ru(bpy)_3^{+}$ is formed by reduction of $Ru(bpy)_3^{2+}$ by the radical, followed by combination of Ru^{I} and Ru^{III} complexes to give $[Ru(bpy)_3^{2+}]^*$ (Rubinstein and Bard, 1980), which emits light at 610 nm. $Ru(bpy)_3^{2+}$-labeled DNA using a sacrificial reductant to produce ECL has been developed as the basis of a very sensitive method to detect oligonucleotide hybridization (Leland and Powell, 1990; Blackburn *et al.*, 1991; Xu and Bard, 1995).

The polymer $[Ru(bpy)_2(PVP)_{10}]^{2+}$ (Ru-PVP, PVP = polyvinylpyridine) shown in Fig. 13.5 can be used for "reagentless" DNA sensors since it can be electrochemically activated to react with DNA in films and generate ECL directly (Dennany, Forster and Rusling, 2003). That is, DNA itself is the sacrificial reductant, removing the need for an external sacrificial reductant in DNA detection. ECL can be measured from a single sensor by positioning an optical fiber under an electrode coated with a Ru-PVP/enzyme/DNA film, and directing the light to a photomultiplier tube. This type of sensor allows the simultaneous recording of voltammetric and ECL signals (Dennany, Forster and Rusling, 2003; So *et al.*, 2007). While these sensors are excellent for exploratory studies, high-throughput analysis requires an array format.

The chemistry of the detection process is summarized in Scheme 13.2. ECL is generated from guanine moieties present on DNA strands in the films (Dennany, Forster and Rusling, 2003). Electrochemical oxidation generates Ru^{III}-PVP, and guanine radicals are initially formed (Eq. 13.3) by catalytic oxidation of guanines (Eq. 13.4). These guanine radicals can react with the metallopolymer (Eq. 13.5) to produce electronically excited Ru^{II}* sites in the film (Eq. 13.6). Alternatively, Ru^{I}-PVP can be formed from reaction of Ru^{II}-PVP with $G^{\bullet}$, and can then react with Ru^{III}-PVP to produce the excited Ru^{II}* state to give ECL. As in purely electrochemical detection of DNA damage, catalyst active sites gain better access to guanines in partly unfolded, damaged DNA than in intact ds-DNA, thus increasing the rate of the catalytic process and consequently the output of ECL light.

ECL is well suited to arrays without individually addressable electrodes. An ECL array can be spotted directly on a conductive plate, for example, a single pyrolytic graphite (PG) block electrode. We have developed convenient, prototype high-throughput toxicity screening arrays based on multiple spots of DNA, enzyme, and the Ru-PVP polymer (Fig. 13.5). Up to 50 individual spots, each an LbL film containing DNA, enzyme, and Ru-PVP, can be manually micropipetted onto the 1×1 in. array plate. We are also evaluating automated spotting devices that can be used to deposit hundreds of spots on similar arrays.

As in the single probe sensors, the enzyme reaction is run first on this array, which then is washed and placed into an electrochemical cell housed in a dark box with a CCD camera (Fig. 13.6) (Hvastkovs *et al.*, 2007). Upon application of 1.25 V versus

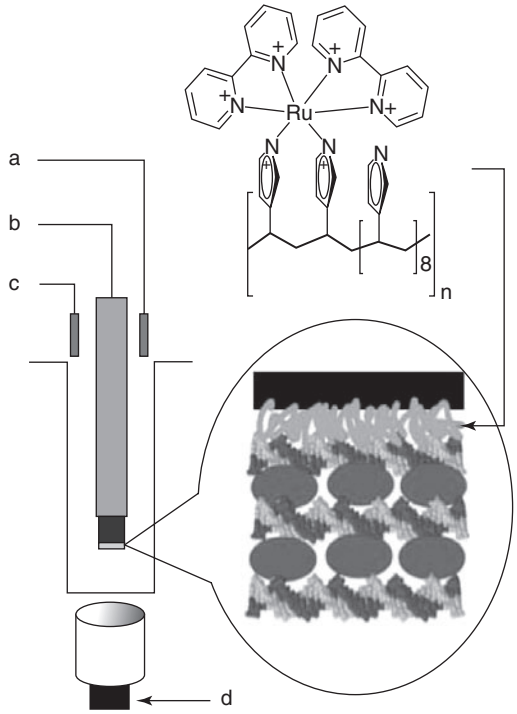

Figure 13.5 Sensor system for simultaneous ECL and voltammetry detection. The reference electrode **(a)**, working electrode **(b),** and Pt counter electrode **(c)** are located in a glass cell with an extended cylindrical glass base. A fiber optic cable **(d)** is positioned on the outside of the cell directly under the sensor surface and leads to a photomultiplier tube. Ru-PVP (structure shown), DNA (brown), and enzyme (blue) layers forming the active sensor film are shown on the right. Only one layer of RuPVP is shown on the sensor, although several can be used to enhance S/N.

$$Ru^{II}\text{-PVP} \leftrightarrow Ru^{III}\text{-PVP} + e^{-}\,(\text{at electrode}) \tag{13.3}$$

$$Ru^{III}\text{-PVP} + G \rightarrow Ru^{II}\text{-PVP} + G^{\bullet} + H^{+} \tag{13.4}$$

$$G^{\bullet} + Ru^{III}\text{-PVP} \rightarrow G_{2ox} + Ru^{II*}\text{-PVP} \tag{13.5}$$

$$Ru^{II*}\text{-PVP} \rightarrow Ru^{II}\text{-PVP} + h\nu\,(610\text{ nm}) \tag{13.6}$$

17 **Scheme 13.2** ••.

3 SCE, the electrochemical oxidation of Ru-PVP initiates the measurement chemistry in Scheme 13.2 and generates light from each spot, which is measured with the CCD camera over an integration time of ~20 seconds. As in all catalytic DNA detection schemes, larger signals are obtained from damaged DNA because of better accessibility of the guanines to the catalyst as the ds-DNA unravels.

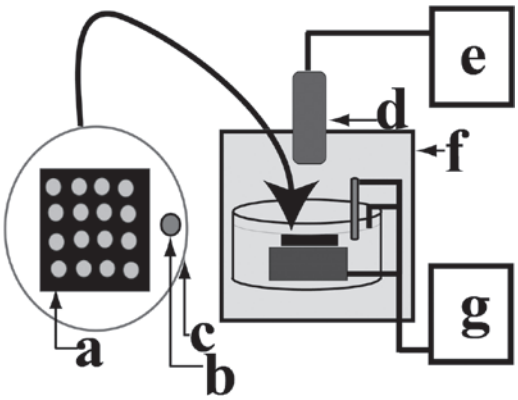

Figure 13.6 ECL arrays for toxicity screening: **(a)** array, **(b)** reference electrode, **(c)** counter electrode, **(d)** CCD camera, **(e)** computer, **(f)** dark box housing, and **(g)** potentiostat to apply voltage for ECL generation. Adapted with permission from Hvastkovs *et al.* (2007). Copyright 2007 American Chemical Society.

ECL arrays can be configured to measure the time course of reactions catalyzed by a single enzyme, or can contain a collection of enzymes for simultaneous comparison of reactive intermediate formation kinetics. Results can be reorganized and presented in a number of ways by computer software. Figure 13.7 shows an ECL array with 49 RuPVP/DNA/enzyme spots designed to study rates of DNA damage for the bioactivation of B[*a*]P by the human enzyme cyt P450 1B1. Individual array spots were subjected to 0.5-mM H_2O_2 and 100-μM B[*a*]P for various times marked on the figure. We can see that light intensity increased with the time of the enzyme reaction. Control spots were exposed to B[*a*]P alone or H_2O_2 alone, and showed little change in ECL. These controls are necessary to confirm that H_2O_2 activates the enzymes but does not damage DNA. Figure 13.7b illustrates a useful way of expressing the array data, as a plot of the final/initial ECL ratio.

Figure 13.8 illustrates oxidation of B[*a*]P with five enzymes in a single array (Hvastkovs *et al.*, 2007). The data have been rearranged by computer software so that representative spots for a single enzyme lie in a specific row. Relative rates of DNA damage were estimated simultaneously in this way for these five enzymes in ~1 minute of enzyme reaction time and 20 seconds of array development time. The slopes of the linear ECL increases correlate with DNA damage rates, and are compared in the graph on the right of Fig. 13.8. Bioactivation producing DNA damage taken as the initial slopes of these graphs was in the order cyt P4501B1 > cyt P4501A2 > cyt $P450_{cam}$ > cyt P4502E1 > Mb, the same as the order of relative metabolic activity of these enzymes toward B[*a*]P (Hvastkovs *et al.*, 2007). The slope of the linear ECL increase estimates the relative activity of different enzymes to produce reactive metabolites.

We have also developed and tested ECL arrays for *N*-nitrosamines (Krishnan *et al.*, 2007). Nitrosamines have been reported to be carcinogens in more than 30 species (Hecht, 1998). Cyt P450s, in particular CYP2E1, bioactivate *N*-nitrosamines to reactive intermediates, mainly by α-hydroxylation. *N*-Nitrosopyrrolidine (NPYR) (Preussmann and Stewart, 1984) was used as the test compound. Adducts form from reaction of DNA with NPYR metabolites (Scheme 13.3) (Wang *et al.*, 2001).

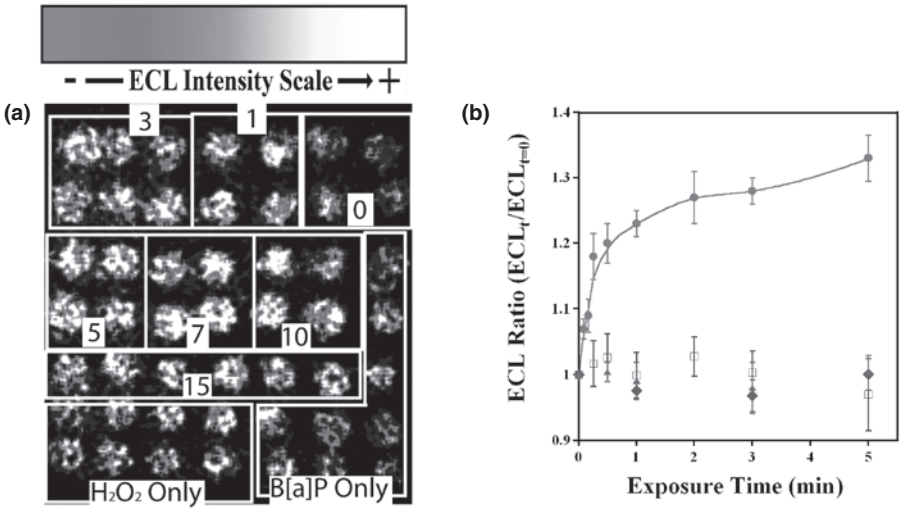

Figure 13.7 **(a)** CCD image of ECL array with 49 individual RuPVP/DNA/enzyme spots all containing cyt P450 1B1. Boxes denote spots that were exposed to 0.5-mM H_2O_2 + 100-μM B[*a*]P for the labeled times (min). Controls (bottom) were exposed to B[*a*]P or H_2O_2 only for increasing amounts of time from 1 to 7 minutes as viewed from right to left (not marked for clarity). **(b)** ECL ratio plot demonstrating the increase in ECL intensity versus time of enzyme reaction. Controls show ECL response versus time exposed to B[*a*]P only (blue squares), H_2O_2 only (green diamonds), and 0.5-mM H_2O_2 + 100-μM B[*a*]P + 30 μM of inhibitor αNF (purple triangles). Adapted with permission from Hvastkovs *et al.* (2007). Copyright 2007 American Chemical Society.

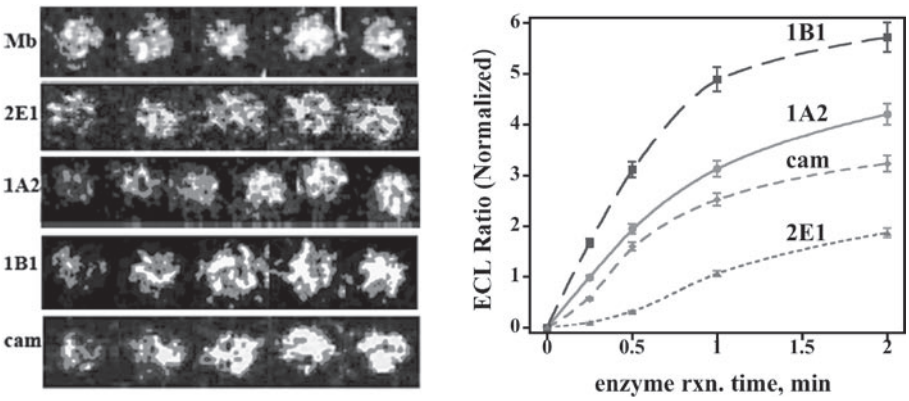

Figure 13.8 ECL array results for enzyme reactions with 100-μM benzo[*a*]pyrene + 0.5-mM H_2O_2 **(a)** reconstructed images for reaction times of 0, 1, 3, 5, and 7 minutes for cyt P450 enzymes and myoglobin on the same array. CCD images are recolorized with the brighter spots showing more DNA damage. **(b)** ECL initial/final ratios normalized for the amount of enzyme in each spot. Adapted with permission from Hvastkovs *et al.* (2007). Copyright 2007 American Chemical Society.

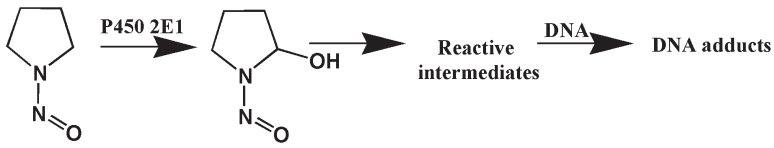

18 **Scheme 13.3** ••.

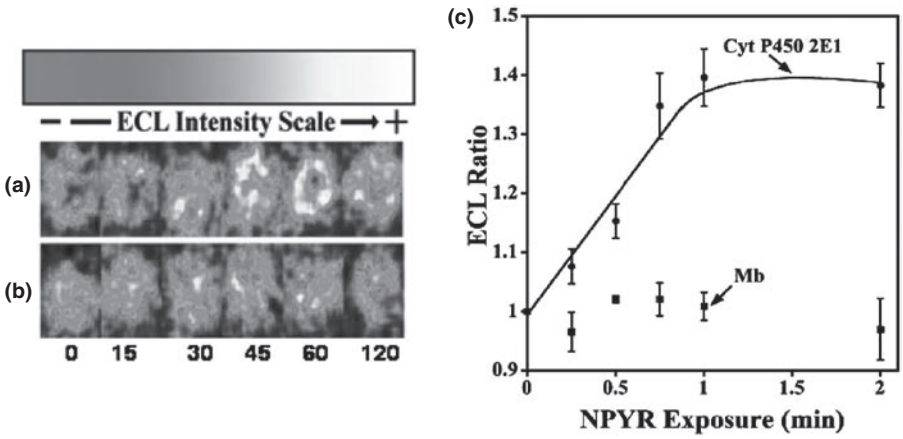

Figure 13.9 ECL array data after exposure to NPYR: **(a)** digitally reconstructed image demonstrating CCD-captured ECL emitted from RuPVP/DNA/cyt P450 2E1 array and **(b)** RuPVP/DNA/Mb array exposed to 150-μM NPYR + 1-mM H_2O_2 for the denoted amounts of time (s). **(c)** Ratio plot demonstrating the ECL signal increase from films containing cyt P450 2E1 or Mb. Adapted with permission from Krishnan *et al.* (2007). Copyright 2007 Royal Society of Chemistry.

Reconstructed ECL arrays (Krishnan *et al.*, 2007) show the ECL response when the DNA/cyt P450 2E1 and DNA/Mb films are exposed to increasing times of damage solution (Fig. 13.9a,b). Each spot contains enzyme, DNA, and RuPVP. The increase in light intensity with time of the Cyt P450 2E1 reaction indicates increased DNA damage via generation of a reactive intermediate. No change in ECL occurred for RuPVP/DNA/Mb spots, showing that Mb does not bioactivate NPYR. Figure 13.9c shows the ECL data in the ratio plot format, and is another way to present the result that cyt P450 2E1 bioactivates NPYR, but Mb does not.

The future vision for this ECL toxicity arrays includes screening for the formation of reactive intermediates (Krishnan *et al.*, 2007; Rusling, Hvastkovs and Schenkman, 2007; So *et al.*, 2007), identifying the enzymes producing them (Wang *et al.*, 2005; Hvastkovs *et al.*, 2007), and applications in drug–drug interactions involving enzyme inhibition (Mugweru and Rusling, 2006). For this type of array, we will need also to utilize phase II and multienzyme metabolic reaction in the arrays. This development is currently under way in our laboratories.

We can also use liver microsomes as enzyme sources in the arrays. Figure 13.10 shows a digitally reconstructed image of an array in which each spot contains DNA,

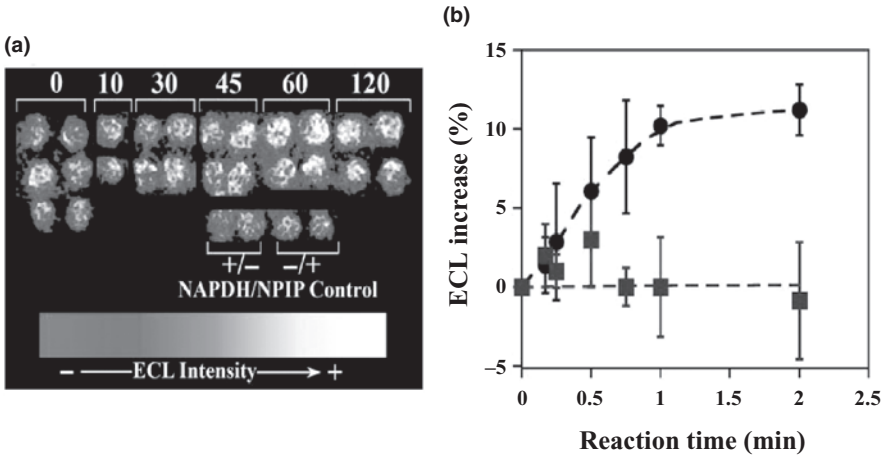

Figure 13.10 Data from ECL arrays using rat liver microsomes (RLMs) as the enzyme source. **(a)** Reconstructed image showing the results of an array exposed to NADPH and 1-mM NPIP for increasing times (in seconds at top). Spot had film architecture $(DNA/RuPVP)_2DNA(RuPVP/RLM/DNA)_3$. Controls (bottom) were exposed to only NPIP in buffer or NADPH alone. **(b)** ECL percentage change versus reaction time (black circles) demonstrating from array runs. Controls (blue squares) correspond to spots incubated in NPIP (no NADPH) under the same conditions.

rat liver microsomes (RLMs), and RuPVP. The spots were exposed to an NADPH-generating system containing 1-mM *N*-nitrosopiperidine (NPIP) for increasing amounts of time at 37 °C. NPIP is a known genotoxic nitrosamine compound that induces esophageal and liver tumors after exposure (Young-Scaime *et al.*, 1995). The use of liver microsomes allows the cyt P450 enzymes in the array to be activated by the natural *in vivo* route (Scheme 13.1) through electron transfer from NADPH via with cyt P450 reductase (CPR) (Ortiz de Montellano, 2005). NPIP is metabolically activated by the cyt P450 enzymes present in the RLM and diffuses through the films to react with nucleophilic DNA. Figure 13.10 shows the increase in ECL intensity with reaction time. Figure 13.10 also shows control experiments where spots were incubated with only NPIP in buffer (no NADPH) or the NADPH system alone. Controls show negligible ECL increases. The relative turnover for NPIP was found by dividing the initial slope of the ECL plot by the amount of RLM present in the film estimated by a quartz crystal microbalance (QCM). For this example, turnover rate was 660 min^{-1} (mg RLM)$^{-1}$.

13.3 DNA/ENZYME BIOCOLLOIDS FOR LC-MS TOXICITY SCREENING

Progress in techniques like electrospray ionization (ESI) and matrix-assisted laser desorption ionization (MALDI) has made MS unprecedented in popularity for bio-analysis. ESI has facilitated coupling of capillary liquid chromatography (capLC) to MS (Vanhoutte *et al.*, 1997; Appruzzese and Vouros, 1999; Gangl, Turesky and Vouros, 2001), minimizing the need to isolate and purify DNA adduct samples and facilitating small sample size and ultrahigh sensitivity in detection of nucleobase adducts (Tarun

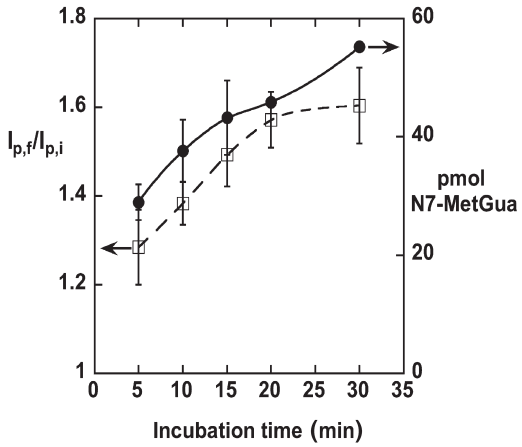

Figure 13.11 Comparisons of electrochemical toxicity sensor with nucleobase adduct formation rate. Peak current ratio $I_{p,f}/I_{p,i}$ (final/initial) for sensors consisting of $(PDDA/DNA)_2$ films on graphite electrode-based (□), and pmol *N*7-methylguanine found by LC-MS (•) of hydrolyzed DNA from similar films on carbon cloth. Both assays after incubation of DNA films with 2-mM MMS. Adapted with permission from Tarun and Rusling (2005b). Copyright 2005 American Chemical Society.

and Rusling, 2005a). LC-MS methods are among the most specific and versatile methods to detect DNA adducts, and can provide chemical structures and rates of formation of specific nucleobase adducts.

In the early days of developing toxicity sensors, we used LC-MS to measure DNA adducts to confirm that the sensors actually detect DNA damage (Zhou *et al.*, 2003; Tarun and Rusling, 2005b). We measured rates of altered nucleobases by LC-MS using DNA films on carbon cloth that had been reacted with damage agents and hydrolyzed (Yang, Wang and Rusling, 2005; Tarun and Rusling, 2006). In an early example, response of electrochemical toxicity sensors gave good correlations with the rate of formation of *N*-7-methylguanine found by LC-MS after incubation with methyl methane sulfonate (MMS) (Fig. 13.11) and epoxides. Such correlations provided direct evidence that the slopes of sensor response versus enzyme reaction time measure relative rates of DNA damage. Sensor and LC-MS results also correlated well with animal genotoxicity estimated by carcinogenicity index TDL_o in rodents (Tarun and Rusling, 2005b, 2006).

Preliminary results showed that films of enzymes and DNA similar to those used in the arrays could provide nucleobase adducts for LC-MS detection after running the enzyme reaction. These early films for LC-MS were made on carbon cloth, but we later found that increased reaction rates resulting in more sensitive adduct detection could be effected when the films were made on 500-nm-diameter silica colloids. We shall see in the succeeding discussion that these enzyme/DNA biocolloids combined with neutral hydrolysis of the DNA, and capLC-MS with online sample preconcentration provides a very rapid and sensitive method for measuring and identifying reactive metabolites that may be involved in genotoxicity. Together, ECL arrays and capLC-MS analyses provide complementary tools for toxicity studies. The ECL arrays are rapid, inexpensive, high-throughput screening tools, while the capLC-MS approach is a bit more

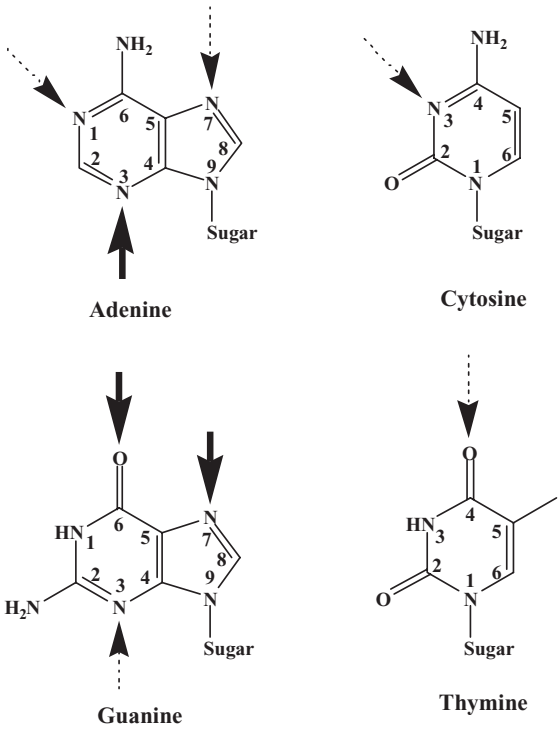

Scheme 13.4 Sites of DNA alkylation subject to attach by reactive drug metabolites. Arrows show major (bold, solid arrow) and minor (broken arrow) alkylation sites.

time-consuming and costly, but provides a wealth of information on reactive intermediates, their nucleobase adducts, and the rates of formation of these products.

Before we describe specific DNA/enzyme biocolloids, we digress to summarize basic DNA chemistry necessary for understanding their operation. Many DNA adducts are formed by alkylating agents (Marnett and Burcham, 1993), and nitrogen and oxygen atoms on nucleobases are active sites (Scheme 13.4). Reactive metabolites are often good alkylating agents or electrophiles and react at one of these nucleophilic sites on the bases (Scheme 13.5). In practice, guanine is the most reactive base. An example of an *N*7-guanine adduct is shown in Scheme 13.6.

Scheme 13.5 also illustrates the useful sample preparation method of neutral thermal hydrolysis, which selectively ejects damaged DNA nucleobases. Alkylation at *N*7-guanine and *N*3-adenine makes the *N*-glycosidic bonds thermally labile for G and A derivatized at these positions (Zamenhof and Arikawa, 1966; Zoltewicz and Clark, 1972). Thus, simple heating of damaged DNA produces a sample enriched in *N*7-guanine- and *N*3-adenine adducts, with a much smaller fraction of native nucleobases than would be obtained by acid or enzymatic hydrolysis (Jacoby, 1980; Tarun and Rusling, 2005b). For this reason, neutral thermal hydrolysis is an excellent sample preparation method for LC-MS.

The use of nanoparticles for biocatalysis was pioneered by Lvov and Caruso (Caruso *et al.*, 1998; Caruso and Möhwald, 1999; Caruso and Schüler, 2000; Lvov and Caruso,

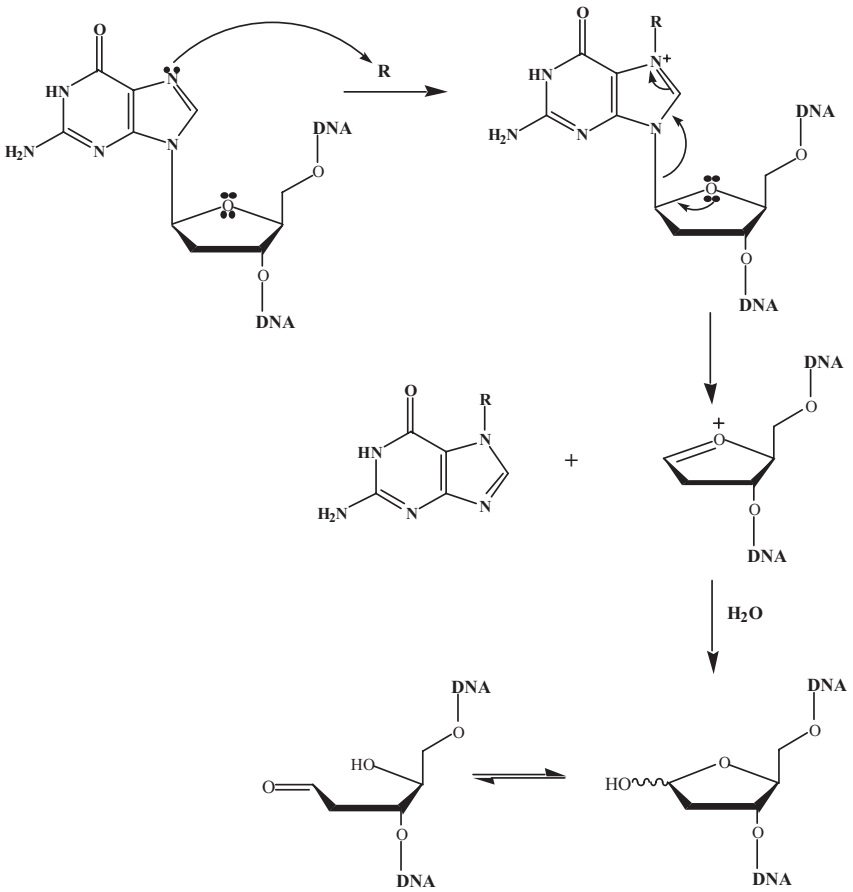

Scheme 13.5 Mechanism of *N*7-alkylation of guanine and subsequent depurination of the damaged nucleobase that can be effected by neutral thermal hydrolysis. R = electrophilic reactive metabolite.

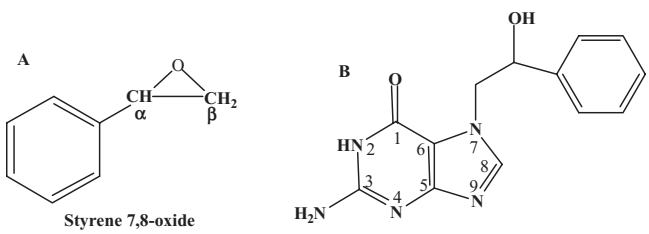

Scheme 13.6 An example of an *N*7-guanine adduct formed from reaction of the styrene metabolite styrene 7,8-oxide with guanine moieties in DNA.

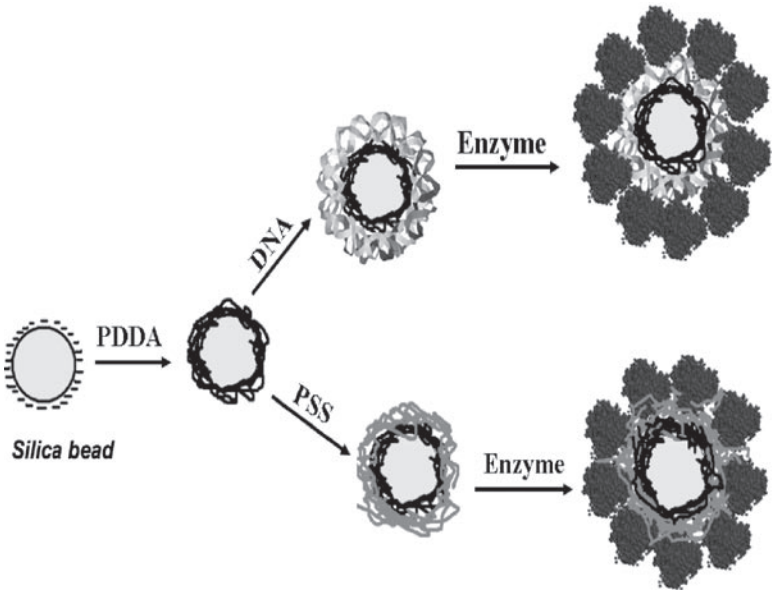

Scheme 13.7 Conceptual illustration of DNA/enzyme film formation on silica microbeads. Layer-by-layer electrostatic assembly is employed to immobilize positively charged PDDA on the negatively charged microbeads, followed by sequential adsorption of negatively charged poly(styrene sulfonate) (PSS) or DNA, and a positively charged enzyme layer (blue circles).

4 2001; Fang *et al.*, 2002; Shutava *et al.*, 2004). They used alternate electrostatic layer-by-layer (LbL) film assembly (Lvov, 2000, 2001; Ariga, Hill and Ji, 2007; Zhang, Chen and Zhang, 2007), the same method used for our sensor arrays, to form active enzyme films of glucose oxidase, horseradish peroxidase, and urease on spherical nanoparticles. Enzyme and DNA/enzyme *biocolloids* for reactive intermediate screening are illustrated in Scheme 13.7. Their tiny size offers a very large active surface area and the ability to employ tiny solution volumes to conserve enzyme and obtain more product per unit time for subsequent determination of major and minor products of both the enzyme and DNA reactions.

To demonstrate the biocolloid approach, we show results for styrene oxide and 4-(methylnitrosoamino)-1-(3-pyridyl)-butanone (NNK) oxidized using human cyt P450
5 2E1 (CYP 2E1) (Bajrami *et al.* , submitted). Cyt P450 2E1 is a prime catalyst in the metabolism of styrene to styrene oxide (Scheme 13.6) *in vivo* (Tanaka, Terada and Misawa, 2000). NNK is an *N*-nitroso procarcinogen in tobacco smoke that has been implicated in cancer risk (Scheme 13.8) (Hecht, 2003; Wang *et al.*, 2003). Styrene and NNK were oxidized with cyt P450 2E1 biocolloids activated by 1 mM H_2O_2. Styrene forms styrene oxide exclusively from the enzyme reaction, while metabolites of NNK undergo hydrolysis to 4-hydroxy-1-(3-pyridyl)-butanone (HPB) (Wang *et al.*, 2003) (Scheme 13.8). Figure 13.12 shows styrene oxide and HPB production as detected by
6 GC for styrene oxide and LC-MS for HPB. The rate of production of both metabolites was initially similar, but over 5 minutes the rate of styrene oxide production was larger than that of HPB.

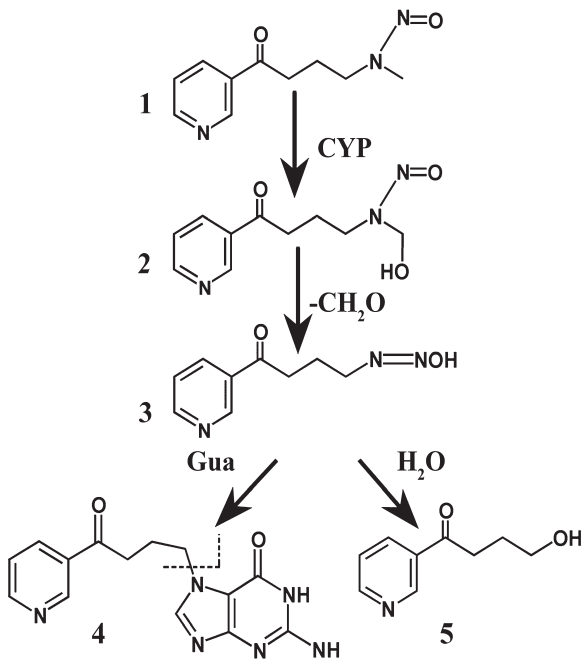

Scheme 13.8 Pathway for cyt P450 (CYP)-catalyzed bioactivation of NNK **(1)** (Wang *et al.*, 2003), which undergoes α-hydroxylation to unstable intermediate **(2)** that loses formaldehyde to form 4-oxo-4-(3-pyridyl)-1-butanediazohydroxide **(3)**. Reaction of **3** with guanine produces several adducts including pyridyloxobutylation at *N*7 (**4**, 7-[4-oxo-4-(3-pyridyl)but-1-yl]Gua). Hydrolysis of **3** produces 4-hydroxy-1-(3-pyridyl)-1-butanone (HPB, **5**). The dashed line in **4** represents fragmentation in MS.

Figure 13.13 shows data for DNA adducts obtained from NNK metabolites made using DNA/cyt P450 2E1 biocolloids. Figure 13.13a is the capLC/MS-MS chromatogram and 13b is the SRM spectrum showing the product m/z peaks after reaction and neutral thermal hydrolysis. The m/z 299 → 52 is consistent with the previously reported pyridyloxobutylation of guanine via attachment at the most likely *N*7 location in Scheme 13.8 (Wang *et al.*, 2003), which shows an *N*7-pyridyloxobutylated guanine that would produce m/z 152 (Gua) upon fragmentation.

The multiple peaks in Fig. 13.13a are probably due to several positional isomers (Wang *et al.*, 2003), since monitoring at this m/z also detects adducts with linkages at positions other than *N*7 of guanine. The m/z 299 peaks for the hydrolysate are consistent with the formation of pyridyloxobutyl-guanine from the enzyme-catalyzed oxidation of NNK.

In this case, HPB is not the DNA-reactive metabolite. The precursor to HPB is a short-lived species that reacts with DNA (**3**, Scheme 13.8). Figure 13.13c shows that the integrated area of this peak increases linearly similar to HPB in Fig. 13.12. Thus, rate of formation of the specific metabolite produced directly mirrors the rate of formation of the major DNA adducts in the films.

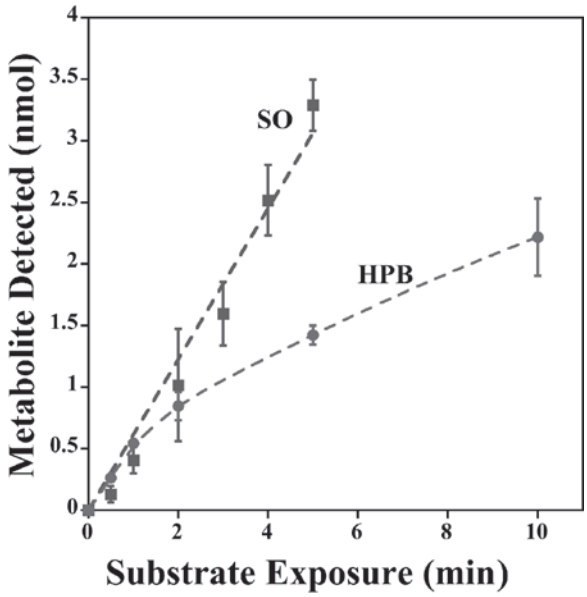

Figure 13.12 Influence of reaction time on amount of styrene oxide (SO, blue squares) from 1% styrene and HPB (red circles) from 100-mM NNK found from reaction with PSS/cyt P450 2E1 colloids activated by 1-mM H_2O_2 in pH 5.5 buffer. Adapted with permission from Bajrami *et al.* (••). Copyright 2007 American Chemical Society.

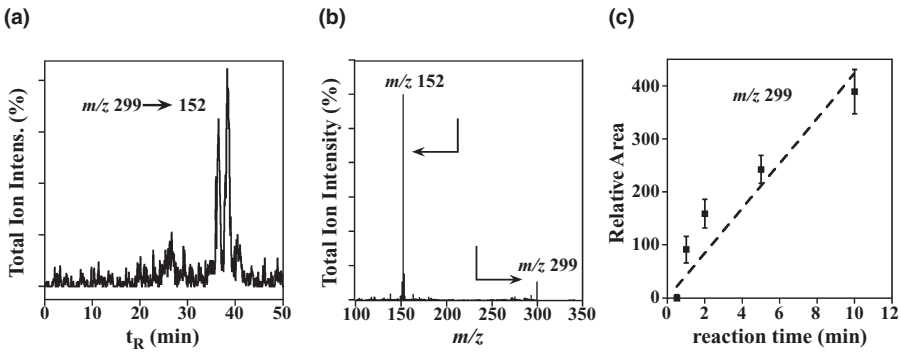

Figure 13.13 CapLC/MS-MS results for NNK reaction catalyzed by DNA/cyt P450 2E1 microbeads in pH 5.5 buffer. **(a)** Chromatogram after a 15-minute reaction. **(b)** Mass spectrum analyzed by SRM (m/z 299 → 152) of same sample as in panel a. © Influence of reaction time on total integrated area of the peaks in panel a at t_R = 37. Adapted with permission from Bajrami *et al.* (••). Copyright 2007 American Chemical Society.

These results show that DNA/enzyme biocolloids can be used to measure formation rates and confirm structures of both metabolites and DNA adducts. This technique can be used for substrates that do not produce DNA adducts as well as those that do, and can thus be used in other chemical and drug discovery studies such as enzyme inhibition. Finally, we have recently made biocolloids that employ liver microsomes

and microsomes genetically engineered to contain a single cyt P450 enzyme and its reductase, so that tedious purification of individual enzymes can be avoided. These microsome biocolloids contain cyt P450 reductase and can be activated with NADPH, exactly as in conventional biocatalysis with microsomes (Krishnan *et al.*, in preparation).

13.4 ALTERNATIVE ARRAYS AND OTHER NOVEL APPROACHES

The distillation of vast numbers of potential lead drug candidates involves initial screening of prospective hit molecules for possible toxicity that might be missed in later *in vivo* tests. Such *in vitro* screens include those for genotoxicity, hERG channel block, drug–drug interactions, and metabolite-mediated toxicity. In addition, these assays often include a standard cytotoxicity (cell destruction) assay (Kramer, Sagartz and Morris, 2007). These assays must be able to detect potential toxicity from thousands of potential candidates in a high-throughput and cost-efficient manner, which is not always realized. In addition, as significant monetary losses in pharmaceutical development occur upon late stage discovery of toxicity, preliminary *in vitro* screens must selectively and sensitively identify toxic candidates while keeping those deemed acceptable in the development pipeline (Nicholson *et al.*, 2002).

13.4.1 Traditional Cell-Based Toxicity Detection

Typically, initial *in vitro* toxicity assays are designed to monitor degrees of cytotoxicity arising from exposure to a compound of interest. Cytotoxicity is typically induced via some form of DNA damage, or genotoxicity (Kramer, Sagartz and Morris, 2007). The bacterial reverse mutation mutagenicity assay (Ames test) (Ames, Mcann and Yamasaki, 1975), the SOS/*umu* test (Oda *et al.*, 1985; Liebler and Guengerich, 2005), the micronucleus test (MNT) (Galloway *et al.*, 1994), the chromosomal aberration (CA) test, the mouse lymphoma assay (MLA) (Kramer, Sagartz and Morris, 2007), and the Comet assay (Singh *et al.*, 1998; Sasaki *et al.*, 2000) for chromosome breakage are currently employed as indirect genotoxicity screens for potential drug candidates and environmental contaminants. The most well known is the Ames test that assays the ability of a compound to induce frame or base pair shifts that facilitate the growth of a bacterial strain in the absence of certain amino acids (Ames, Mcann and Yamasaki, 1975). These assays predominantly measure cell growth, protein expression, or, in the case of the Comet assay, the electrophoresis gel tail length (Singh *et al.*, 1998), to gauge relative genotoxicity. The desirable quality of these tests is that predefined thresholds provide *yes*/*no* answers to facilitate developmental decisions. In cases generating a "yes" toxicity answer, the tested compound may be shelved or redesigned unless a certain amount of genotoxicity is tolerated, for instance in cancer drug development (Kramer, Sagartz and Morris, 2007). Despite their ubiquitous and required use, generally these tests have low specificity providing negative output for certain classes of compounds, such as aneugens (aneuploidy inducing), or give false positives upon exposure to non-genotoxic compounds (Hastwell *et al.*, 2006).

High-throughput modifications to these mutagenicity and clastogenicity (chromosome breakage) tests have been reported, typically employing microtiter plate formats (Kramer, Sagartz and Morris, 2007). For instance, the use of such a platform imparts a bit of high-throughput nature to the electrophoresis-based Comet (Kiskinis, Suter and Hartmann, 2002) and bacterial mutagenesis Ames II assays (Flukiger-Isler *et al.*, 2004).

Laser scanning cytometry allowed for more rapid analysis of stained erythrocytes in the MNT assay (Styles *et al.*, 2001). A similar detection approach was employed using bone marrow cells in an *in vitro* approach to the MNT assay (Shuga *et al.*, 2007). However, newer genotoxicity screens designed to improve upon the traditional Ames assays have yet to attract significant mainstream industrial attention due to high throughput or specificity limitations (Van Gompel *et al.*, 2005).

Employing a fusion plasmid coupling genes for green fluorescent protein (GFP) to growth arrest and DNA damage (GADD) protein, Hastwell *et al.* demonstrated higher specificity and comparable sensitivity in determining a host of genotoxic agents compared with the Ames test (Hastwell *et al.*, 2006). In addition, the GADD-GFP assay was able to determine the action of aneugens, which the Ames assay cannot. These benefits were hypothetically due to the eukaryotic nature of the assay and the importance of the p53-binding motif designed into the GADD protein. Due to the removal of DNA repair mechanisms in the bacterial strains for Ames assays, some relatively benign xenobiotics produced characteristic false-positive outputs. The GADD-GFP system accounted for these false positives presumably due the use of repair-oriented p53 competent cells in the system (Hastwell *et al.*, 2006).

13.4.2 Metabolite Screening

Another important aspect for *in vitro* toxicity screening is the consideration that many compounds administered *in vivo* are toxic upon metabolism (bioactivation) (Oda *et al.*, 1985; Kramer, Sagartz and Morris, 2007). A common drawback that exists in the typical mutagenicity/toxicity screens is that addition of exogenous liver homogenate (S9 fraction) is necessary to account for reactive metabolite genotoxicity. Indeed, throughput in the aforementioned GPDD-GFP test was hampered by this modification (Hastwell *et al.*, 2006). Although the addition of a liver fraction introduces a variety of enzymes involved in general metabolism, no information is garnered regarding enzyme specificity or mechanism. In an attempt to ascertain such information in toxicity screening, purified or microsomal preparations of cyt P450 enzymes in conjunction with cell lines have been incorporated. Arrays of cyt P450 3A4 and 2D6 sol-gel immobilized in contacting a MCF7 breast cancer cell monolayer were used to determine metabolite efficacy in promoting cytotoxicity. Scheme 13.9 demonstrates the metabolite enzyme toxicity analysis chip (MetaChip) technology, which involves suspending cyt P450 enzymes in a sol-gel mixture and clamping the sol-gel to a monolayer of cells. Cytoxan and Tegafur were metabolized by the immobilized cyt P450s, the respective reactive metabolites diffused into the proximal cancer cells, and cell viability was measured by fluorescence after cell staining (Lee *et al.*, 2005b).

Overexpression of cyt P450 3A4 in supersomes and liver cells has also been exploited to screen for metabolite toxicity. The toxicity of several drugs with known adverse drug reactions (ADRs) toward the HepG2 cell line was reported with cell viability measured using MTT colorimetric and ATP chemiluminescent assays. Ketoconozole inhibition elucidated the action of the particular P450 isoform in the metabolism of these drugs (Vignati *et al.*, 2005). Idiosyncratic drug reactions (IDRs) were studied employing a proteomics approach where a mixture of drugs causing hepatotoxicity *in vivo* induced intersecting extracellular protein biomarkers from the cells (Gao *et al.*, 2004). Drug–protein interactions can be studied by hepatocyte or microsomal incubation of a scrutinized compound and radioactive or LC-MS analysis of adducted proteins (Evans *et al.*, 2004). Further metabolite analysis can be done employing LC-MS methods after

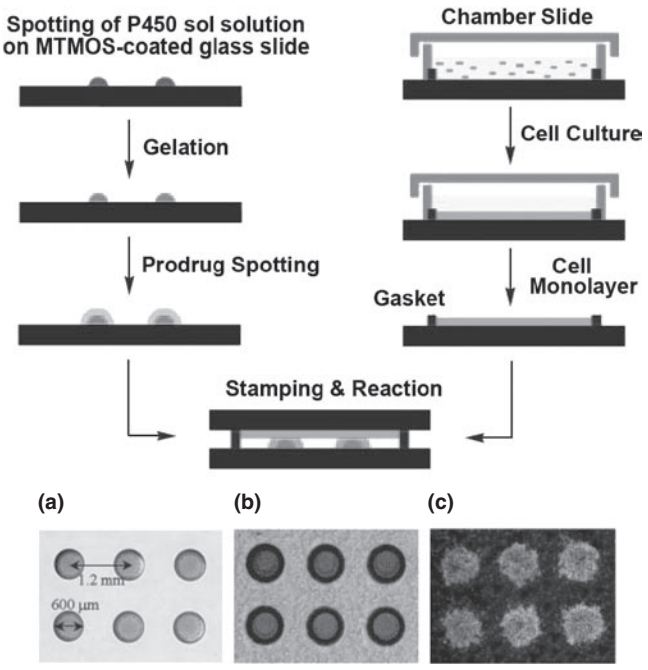

Scheme 13.9 Schematic of the MetaChip platform and microscopic photographs of sol-gel spots. Shown are 30-nL P450 sol-gel spots (**a**), 30-nL sol-gel spots with 60 nL of prodrug solution after being stamped by MCF7 cell monolayer **(b)**, and MCF7 cell monolayer after removal from sol-gel array and staining **(c)**. Adapted with permission from Lee *et al.* (2005b). Copyright 2005 National Academy of Sciences.

adduction or "trapping" with nucleophilic compounds, such as glutathione (Liebler and Guengerich, 2005; Park *et al.*, 2005; Caldwell and Yan, 2006).

Beyond detection of toxicity at the cellular level, several *in vitro* tests have been designed to predict histological (tissue) level toxicity. Inter-organ interactions were modeled using six different organ and tissue cell types placed in the same well of a specially designed microtiter plate connected with a substrate containing common fluid (Li, Bode and Sakai, 2004). *In vitro* modeling of the blood–brain barrier (BBB) has been accomplished employing brain endothelial and glial cells attached in multi-well plates fitted with a porous membrane modeling the capillary barrier. Transfer between the two wells was monitored and can be used to estimate pharmaceutical transfer between capillaries and the brain (Cecchelli *et al.*, 1999). Embryonic stem cells have been used as a screen for potential terotogenic compounds. The embryonic stem cell test (EST) has the ability to accurately determine strong embryotoxic materials. However, this assay needs to be refined to include maternal metabolism enzymes to preclude false positives (McNeish, 2004).

High-content screening (HCS) is a method that measures several cytotoxicity parameters simultaneously. HepG2 hepatocyte cells in 96-well plates were incubated for three days and exposed to several fluorescent dyes to analyze calcium content, mitochondrial membrane potential, DNA content, and cell number. This system was

able to predict the hepatotoxicity of 90% of varying degree liver toxins. Of those, 98% are known to cause some form of *in vivo* toxicity demonstrating the predictive ability of the HCS system (O'Brien *et al.*, 2006).

In order to more accurately model the action of cancerous cell growths, breast cancer cells were encapsulated in alginate poly-L-lysine alginate (ALA) microcapsules and exposed to varying chemotherapeutic drugs. Compared with monolayer culture assays, the studied drugs exhibited altered toxicity profiles in the 3-D microcapsule assay, which demonstrated the complex nature of actual tumor cells and elucidated some serious drawbacks to monolayer cell-based assay formats (Zhang *et al.*, 2005).

13.4.3 -Omics Technologies

Genome sequence alone does not predict disease phenotypes, giving rise to a significant number of approaches designed to analyze gene expression to elucidate such phenotypic outcomes. These fields are termed the -omics fields: genomics (genetic complement), transcriptomics (gene expression), proteomics (cell signaling and protein synthesis), metabolomics (cellular metabolite flux), and metabonomics (endogenous small molecule flux) (Nicholson *et al.*, 2002).

The use of DNA microarrays in transcriptomics or toxicogenomics promises to be a powerful tool in the elucidation of DNA damage mechanism via drug and environmental toxin exposure. In such experiments, selected animals or cell lines are exposed to a compound of interest and after sufficient time, RNA is isolated from the exposed tissue or cells. The RNA is amplified, fluorescently labeled, and allowed to hybridize to array-immobilized DNA probes (Butte, 2002). Additionally, the RNA can undergo reverse-transcription producing the original DNA sequence which can then be analyzed. The overall goal is to determine the regulation of a set of genes due to physiological changes from drug exposure. From a genotoxic standpoint, damage induced by a drug would elicit a damage response from a host of genes that will be detected in the microarray (Ulrich and Friend, 2002). In this fashion, a selection of direct genotoxic agents was discerned from indirect genotoxic agents (i.e. mode of action not directly on DNA itself) based on differences in gene expression profiles after exposure to mouse lymphoma cells (Hu *et al.*, 2004). Gene expression analysis of rat liver cells exposed to a series of marketed thiazolidinedione diabetes drugs was performed to elucidate the IDR mechanism that caused recall of one of the drugs. This method identified several expressed genes involved in DNA damage response, cyt P450 induction, and cell regulatory cycles demonstrating that the IDR response was multifaceted in nature. Also, the DNA expression procedure was able to more sensitively determine IDRs than *in vivo* tests (Vansant *et al.*, 2006).

Microarrays have been employed to measure the damaging effects of electron dosing at 3 eV. Fluorescent DNA microarrays demonstrated that 300 electrons per dT 25-mer oligomer was sufficient to preclude hybridization (Solomun and Sturm, 2007). Overall, despite the promise to elucidate genotoxic mechanism, initial microarray studies have shown less sensitivity than traditional genotoxic assays, such as the MNT assay (Newton, Aardema and Aubrecht, 2004). In addition, questions exist about reproducibility and interpretation, but standardization of protocols can improve interlaboratory findings (Irizarry *et al.*, 2005; Owens, 2005).

Proteomic microarrays have been developed to study translation products in a cellular context. From a toxicity standpoint, the interest lies in the charting of expression levels, emergence of new protein biomarkers, alteration of translated products, or

post-translation modifications (Stoll *et al.*, 2004). For instance, microarrays of capture antibodies have been employed to ascertain the changes in protein expression in cancer cells upon radiation treatment (Sreekumar *et al.*, 2001). Sandwich immunoassay arrays have been developed to quantify several different cellular proteins at femtomolar levels (Schweitzer *et al.*, 2000). Limitations in capture antibody development and high-throughput issues will need to be improved before proteomic microarray applications become more widespread (Stoll *et al.*, 2004).

Metabonomics attempts to study the time flux of relative concentrations of endogenous small molecule components of biofluids and tissues (Lindon *et al.*, 2003). In this fashion, a complete end-point analysis due to genetic expression, protein translation, or metabolite exposure of these samples can be discerned and multiple biomarkers of drug exposure can be elucidated. The benefits of this application are numerous and include a global profiling tool at relatively low per sample expense compared with DNA microarray analysis (Griffin and Bollard, 2004). Magic angle resonance (MAR) ^{1}H NMR allows for histological screening on solid tissue samples after drug exposure. This technique requires little sample workup and does not destroy the sample so that it can be used in multiple analyses (Nicholson *et al.*, 2002; Lindon *et al.*, 2003). Coupled with LC-MS, vast amounts of metabolite and other proteomic biomarker data due to drug exposure can be discerned. An example of metabonomic toxicology was presented by Nicholson *et al.* with the rapid determination of fatty acid metabolism impairment by a failed pharmaceutical candidate. The metabonomic profile of the drug was consistent with several lines of *in vivo* rodent and primate experiments (Mortishire-Smith *et al.*, 2004). Despite high promise, drawbacks of this approach are the throughput and sensitivity of the NMR, the complexity of the data analysis, and initial start-up expenses in acquiring equipment with sufficient frequency resolution. Overall, due to the expense and high-throughput limitations, the -omics fields will likely be used extensively in detailed studies of further developed drug candidates to elucidate findings from preliminary *in vitro* genotoxicity screens (Newton, Aardema and Aubrecht, 2004).

13.4.4 Emerging Toxicity Detection Technologies

In addition to some of the aforementioned cell-based cytotoxicity assays, other novel means of detecting xenobiotic toxicity have also been reported. Cell morphology changes eliciting a transduction signal alteration have shown promise. Scheme 13.10 shows the experimental setup described by Schwartz *et al.* using scattered light intensity changes to monitor real-time cellular viability. Rat hepatocytes were immobilized on a porous silica photonic crystal and upon exposure to cytotoxic agents cadmium chloride or acetaminophen, the intensity of scattered light at 640 nm increased demonstrating the alteration in the cellular structure due to the xenobiotic action (Schwartz *et al.*, 2006).

In a similar vein, microelectrode-containing microtiter plates have been employed to measure the impedance change between the electrode and the ambient upon exposure to cytotoxic agents. Cells adhered to the electrode surface were exposed to various cytotoxic agents that induce morphological changes. Cytotoxicity affects cell viability, cell number, and electrode adherence producing a resistance change from electrode to the surrounding buffer that correlates with rates of xenobiotic-induced cytotoxicity. The results obtained in this fashion charted well with standard colorimetric detection (Xiao and Luong, 2005; Xing *et al.*, 2005; Zhu *et al.*, 2006).

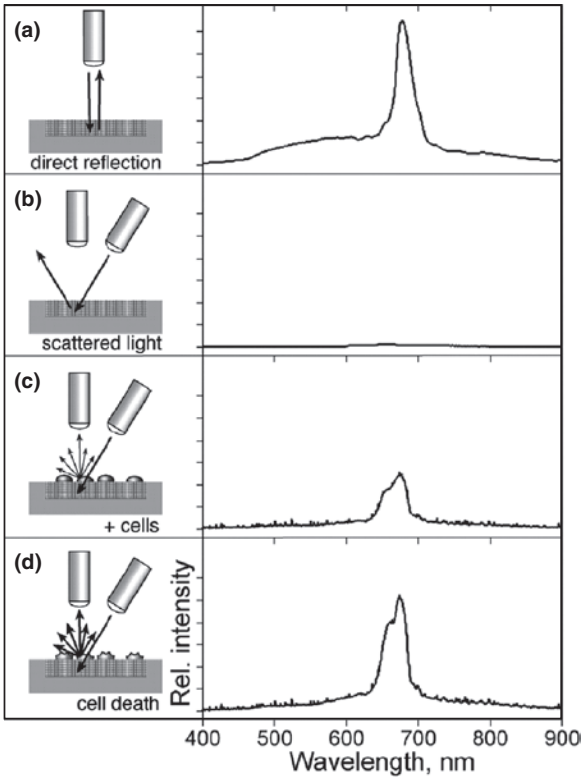

Scheme 13.10 Optical design used to monitor biological events on a polystyrene-filled porous Si photonic crystal, with representative spectra. **(a)** To measure the specular reflection from the photonic crystal, illumination and observation share the same optical path, along the axis normal to the chip surface, leading to a sharp reflectivity peak, as shown on the right of the diagram. **(b)** To measure scattered (diffuse) reflectivity from the photonic crystal, the light source is incident from an off-normal position. The specular reflection from the photonic crystal is no longer observed. **(c)** Placing cells on the surface of the chip introduces scattering centers that direct some of the light into the detection optics. **(d)** Changes in cell morphology alter scattering efficiency, which are detected as changes in the intensity of the spectral peak. Adapted with permission from Schwartz *et al.* (2006). Copyright 2006 American Chemical Society.

Similar electronic microsensors have been employed to monitor certain areas of toxicity upon exposure to exogenous agents. Metabolic oxygen consumption changes and extracellular acidities of tumor cells exposed to drugs were measured concurrently using a multi-parametric electronic sensor. Differences in measured parameters allowed discernment of the mechanism of drug action on the cells (Montrescu *et al.*, 2005). Electrochemical measurement of K^+-induced dopamine release from a microarray of cells demonstrated that exposure to nomifensine, a dopamine transporter inhibitor, can provide a more sensitive toxicity screen than standard staining and counting viable cells (Cui *et al.*, 2006). Also using a microelectrode array format, the decrease in action potentials of cardiac cells was used to estimate the toxicity of pesticides (Natarajan *et al.*, 2006).

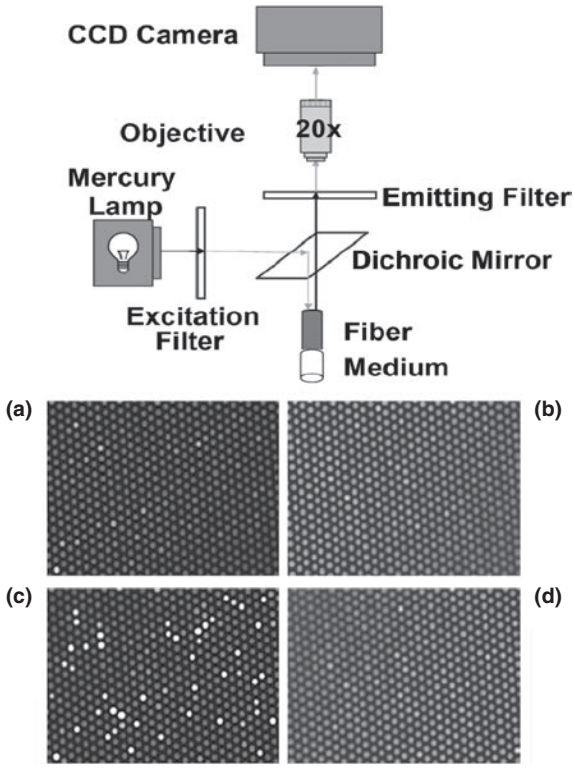

Scheme 13.11 Single-cell array biosensor platform setup and fluorescent images from a small portion of two imaging fiber-based arrays. The left panel shows an array where cells were incubated with medium containing 5 μg mL^{-1} mitomycin C. Fluorescent signals were acquired at **(a)** t = 0 minute and **(b)** t = 90 minutes. The right panel shows the control array where cells were incubated with only medium and fluorescent signals were taken at **(c)** t = 0 minute and **(d)** t = 90 minutes. The bright spots indicate a fluorescence increase, and the cells exposed to MMC were much brighter than the control. Adapted with permission from Kuang, Biran and Walt (2004). Copyright 2004 American Chemical Society.

Other optical detection strategies to monitor toxicity have also been described. Surface plasmon resonance (SPR) has been used to monitor adsorption processes modeling serum-binding behavior of drugs on surfaces (Cooper, 2002). Alveolar epithelial cells anchored to a fiber optic were employed to assay the cytotoxicity of inhalation hazards employing fiber evanescent wave spectroscopy (FEWS). Wavelengths in the mid-IR range were monitored and compared with a MTT colorimetric assay to ascertain damage by various airborne toxic agents (Riley *et al.*, 2006).

Fiber optic arrays to measure genotoxicity were developed by Walt *et al.* employing *Escherichia coli* carrying a *recA:gfp* fusion reporter plasmid. A single bacterium was loaded into a properly sized microwell on the tip of each fiber optic (shown in Scheme 13.11). Bundling of the individual fibers created a high-density biosensor array. Upon exposure to genotoxic medium, fluorescence from expressed GFP was captured

by a distally located CCD camera (Kuang, Biran and Walt, 2004). Likewise, compatible *recA:gfp* and *katG:lux* plasmids inserted into *E. coli* were described to detect and distinguish genotoxic from oxidative cell damage based on increases in fluorescence and bioluminescence, respectively (Mitchell and Gu, 2004a, b). Extending this methodology, *E. coli* containing several different promoters fused with *lux* genes were placed in well plates or constructed chip arrays. Toxicity was assessed from bioluminescence increases detected by a CCD camera and was dependent on reporter gene and employed damage agent (Lee *et al.*, 2005a).

Improvements to the "lab on a chip" concept for biological monitoring continue to be reported. Several unique microfluidic and cell trapping approaches have been described with potential toxicity detection applications (Dittrich and Manz, 2006). *In vitro* protein expression in manufactured oil and water droplets ("biocontainers") was detected fluorescently using a microfluidic approach. Genetic and protein expression components were mixed simultaneously with the oil and water. Expression occurred along a perpendicular reaction strip after mixing, and detection at certain positions along the strip allowed for time-dependent monitoring of protein expression (Dittrich, Jahnz and Schwille, 2005). Also, improvements in such microfluidic devices allow for single-cell immobilization and analysis of the cellular actions upon exposure to an exogenous medium (Dittrich and Manz, 2006). A novel concept in the microfluidics area involves simultaneously monitoring of multiple cell types using a four-compartment flow cell microdevice to mimic *in vivo* metabolism processes. As a test, naphthalene was metabolized in the liver compartment by cyt P450-containing hepatocyte cells followed by flow dispersion into the other compartments of the cell. Depletion of glutathione in the lung compartment denoted reactive metabolite formation (Viravaidya, Sin and Shuler, 2004).

Overall, numerous clever approaches have been explored to measure toxicity of new drug candidates and environmental xenobiotics with varying optical and electrochemical transduction strategies. In order to gain wider acceptance, these platforms must be able to assess chemical toxicity from a wide range of mechanisms in a cost-efficient manner. They must be able to provide more sensitive information, and even chemical structural information, if they are to eventually be used as replacements or in conjunction with traditional toxicity assays. Based on the continual financial driving force to discover toxic pharmaceutical candidates at early stages, we envision that more novel *in vitro* toxicity assays will be developed and employed as initial toxicity screens followed by a more thorough analysis using *-omics* analyses.

13.5 SUMMARY AND FUTURE OUTLOOK

In this chapter, we described new array-based methodology utilizing enzyme/DNA films to screen for reactive drug metabolites based on a DNA-damage end point measured by ECL. Similar enzyme/DNA films on nanoparticles coupled with LC-MS to obtain structure, and rate information for formation of nucleobase adducts and reactive metabolites was also described. Relative rates of DNA damage from both of these biochemical assays can be used to predict relative genotoxicity and the tendency to form reactive metabolites for new drugs. These methods are complementary since the ECL arrays provide rapid screening for reactive metabolites, while the LC-MS approach provides valuable structural and rate of formation information about metabolites and possible nucleobase adducts. Both approaches are adaptable to enzyme inhibition

studies. These technologies are currently being developed in higher-throughput versions taking advantage of modern robotics and biomolecule printing devices that handle sub-nanoliter volumes.

This chapter also surveyed recent developments utilizing other types of array and nanoscience-based technologies for drug toxicity assessment. The future appears bright for incorporation of some of these technologies in high-throughput drug toxicity screening. Many of these approaches could be used alongside or in place of certain conventional toxicity tests.

We feel that the new approaches described herein will prove to be valuable in drug toxicity testing along with other reliable tests and *in silico* assessments. We agree with many pharmaceutical scientists that the future lies in developing predictive batteries of tests upon which to base reliable informed decisions about toxicity at early stages in the development life of a drug (Nasser, Kamel and Clarimont, 2004; Caldwell and Yan, 2006; Mayne, Ku and Kennedy, 2006; Kramer, Sagartz and Morris, 2007). Indeed, this is already happening. We feel that it would be advantageous to evaluate newer, faster, more biochemical-based approaches to the toxicity testing toolbox on an experimental basis, and that perhaps drug companies should develop small groups of bioanalytical scientists charged with this specific task. After a period of evaluation, the new technologies could be adopted if they prove valuable, or discarded if they do not. The hope and dream is that such an approach would establish reliable new high-throughput tests in the toxicity toolbox that would eventually lower the number of drug failures late in the development process, and thus lower drug development costs, as well as drug costs to patients.

10 9 REFERENCES

Adams, C., Adams, P.A. (1992). A comparative study of pH/activity profiles for the anaerobic H_2O_2 and alkyl hydroperoxide supported N demethylation of N methylaniline catalyzed by alkaline haematin and microsomal cytochrome P-450. *J. Inorg. Biochem.*, *45*, 47–52.

Ames, B.N., Mcann, J., Yamasaki, E. (1975). Methods for detecting carcinogens and mutagens with the Salmonella/mammalian-microsome mutagenicity test. *Mutat. Res.*, *31*, 347–364.

Appruzzese, W.A., Vouros, P. (1999). Analysis of DNA adducts by capillary methods coupled to mass spectrometry: a perspective. *J. Chromatogr. B*, *794*, 97–108.

Ariga, K., Hill, J.P., Ji, Q. (2007). ••. *Phys. Chem. Chem. Phys.*, *9*, 2319–2340.

Bajrami, B., Hvastkovs, E.G., Jensen, G., Schenkman, J.B., Rusling, J.F. (••). Enzyme-DNA biocolloids for DNA adduct and reactive metabolite detection by chromatography-mass spectrometry. *Anal. Chem.*, submitted.

Bichara, N., Ching, M.S., Blake, C.L., Ghabrial, H., Smallwood, R.A. (1996). ••. *Drug Metab. Dispos.*, *24*, 112–118.

Blackburn, G.F., Shah, H.P., Kenten, J.H., Leland, J., Kamin, R.A., Link, J., Petermann, J., Powell, M.J., Shah, A., Talley, D.B., Tyagi, S.K., Wilkins, E., Wu, T.-G., Massey, R.J. (1991). ••. *Clin. Chem.*, *37*, 1534–1539.

Bond, J.A. (1989). ••. *CRC Crit. Rev. Toxicol.*, *19*, 227–249.

Butte, A. (2002). The use and analysis of microarray data. *Nat. Rev. Drug Discov.*, *1*, 951–960.

Caldwell, G.W., Yan, L. (2006). Screening for reactive intermediates and toxicity assessment in drug discovery. *Curr. Opin. Drug Discov. Devel.*, *9*, 47–50.

Caruso, F., Lichtenfeld, H., Giersig, M., Möhwald, H. (1998). ••. *J. Am. Chem. Soc.*, *120*, 8523–8524.

11

Caruso, F., Möhwald, H. (1999). ••. *J. Am. Chem. Soc.*, *121*, 6039–6046.

Caruso, F., Schüler, C. (2000). ••. *Langmuir*, *16*, 9595–9603.

Cavalieri, E.L., Rogan, E.G., Devaneshan, P.D., Cremonesi, P., Cerny, R.L., Gross, M.L., Bodell, W.J. (1990). ••. *Biochemistry*, *29*, 4820–4827.

Cecchelli, R., Dehouck, B., Fenart, L., Buee-Scherrer, V., Duhem, C., Lundquist, S., Rentfel, M., Torpier, G., Dehouck, M.P. (1999). In vitro model for evaluating drug transport across the blood-brain barrier. *Adv. Drug Deliv. Rev.*, *36*, 165–178.

Cooper, M.A. (2002). Optical biosensors in drug discovery. *Nat. Rev. Drug Discov.*, *1*, 515–528.

Cui, H., Ye, J., Chen, Y., Chong, S., Sheu, F. (2006). Microelectrode array biochip: tool for in vitro drug screening based on the detection of a drug effect on dopamine release from PC12 cells. *Anal. Chem.*, *78*, 6347–6355.

Dennany, L., Forster, R.J., Rusling, J.F. (2003). Simultaneous direct electrochemiluminescence and catalytic voltammetry detection of DNA in ultrathin films. *J. Am. Chem. Soc.*, *125*, 5213–5218.

Dittrich, P.S., Jahnz, M., Schwille, P. (2005). A new embedded process for compartmentalized cell-free protein expression and on-line detection in microfluidic devices. *Chembiochem*, *6*, 811–814.

Dittrich, P.S., Manz, A. (2006). Lab on a chip: microfluidics in drug discovery. *Nat. Rev. Drug Dev.*, *5*, 210–218.

Ege, D., Becker, W.G., Bard, A.J. (1984). ••. *Anal. Chem.*, *56*, 2413–2417.

Evans, D.C., Watt, A.P., Nicoll-Griffith, D.A., Baillie, T.A. (2004). Drug-protein adducts: an industry perspective on minimizing the potential for drug bioactivation in drug discovery and development. *Chem. Res. Toxicol.*, *17*, 3–16.

Fang, M., Grant, S.P., McShane, M.J., Sukhorukov, G.B., Golub, V.O., Lvov, Y. (2002). ••. *Langmuir*, *18*, 6336–6344.

Flukiger-Isler, S., Baumeister, M., Braun, K., Gervais, V., Hasler-Nguyen, N., Reimann, R., Van Gompel, J., Wunderlich, H.-G., Engelhardt, G. (2004). Assessment of the performance of the Ames II assay: a collaborative study with 19 coded compounds. *Mutat. Res.*, *558*, 181–197.

Friedberg, E.C. (2003). ••. *Nature*, *421*, 436–440.

Galloway, S.M., Aardema, M.J., Ishidate, M., Jr, Ivett, J.L., Kirkland, D.J., Morita, T., Mosesso, P., Sofuni, T. (1994). Report from working group on in vitro tests for chromosomal aberrations. *Mutat. Res.*, *312*, 241–261.

Gangl, E.T., Turesky, R.J., Vouros, P. (2001). Detection of in vivo formed DNA adducts at the part-per-billion level by capillary liquid chromatography/microelectrospray mass spectrometry. *Anal. Chem.*, *73*, 2397–2404.

Gao, J., Garulacan, L., Storm, S., Hefta, S., Opiteck, G., Lin, J., Moulin, F., Dambach, D. (2004). Identification of in vitro protein biomarkers of idiosyncratic liver toxicity. *Toxicol. In Vitro*, *18*, 533–541.

Griffin, J.L., Bollard, M.E. (2004). Metabonomics: its potential as a tool in toxicology for safety assessment and data integration. *Curr. Drug Metab.*, *5*, 389–398.

Guengerich, F.P. (2001). ••. *Chem. Res. Toxicol.*, *14*, 611–650.

Guengerich, F.P., Bell, L.C., Okazaki, O. (1995). ••. *Biochemie*, *77*, 573–580.

Hastwell, P.W., Chai, L.-L., Roberts, K.J., Webster, T.W., Harvey, J.S., Rees, R.W., Walmsley, R.M. (2006). High specificity and high sensitivity genotoxicity assessment in a human cell line: validation of the GreenScreen HC GADD45α-GFP genotoxicity assay. *Mutat. Res.*, *607*, 160–175.

Hecht, S.S. (1998). ••. *Chem. Res. Toxicol.*, *11*, 559–603.

Hecht, S.S. (2003). ••. *Nat. Rev. Cancer*, *10*, 733–744.

Hu, T., Gibson, D.P., Carr, G.J., Torontali, S.M., Tiesman, J.P., Chaney, J.G., Aardema, M.J. (2004). Identification of a gene expression profile that discriminates indirect-acting genotoxins from direct-acting genotoxins. *Mutat. Res.*, *549*, 5–27.

Hvastkovs, E.G., So, M., Krishnan, S., Bajrami, B., Tarun, M., Jansson, I., Schenkman, J.B., Rusling, J.F. (2007). Electrochemiluminescent arrays for cytochrome P450-activated genotoxicity screening. DNA damage from benzo[a]pyrene metabolites. *Anal. Chem.*, *79*, 1897–1906.

Irizarry, R.A., Warren, D., Spencer, F., Kim, I.F., Biswal, S., Frank, B.C., Gabrielson, E., Garcia, J.G.N., Geoghegan, J., Germino, G., Griffin, C., Hilmer, S.C., Hoffman, E., Jedlicka, A.E., Kawasaki, E., Martinez-Murillo, F., Morsburger, L., Lee, H., Petersen, D., Quackenbush, J., Scott, A., Wilson, M., Yang, Y., Ye, Q.S., Yu, W. (2005). Multiple-laboratory comparison of microarray platforms. *Nat. Methods*, *2*, 345–349.

Jacoby, W.B. (ed.) (1980). *Enzymatic Basis of Detoxification*, Vols I and II, Academic, New York.

Kenten, J.H., Casedei, J., Link, J., Lupold, S., Willey, J., Powell, M., Rees, A., Massey, R.J. (1991). ••. *Clin. Chem.*, *37*, 1626.

Kiskinis, E., Suter, W., Hartmann, A. (2002). High throughput Comet assay using 96-well plates. *Mutagenesis*, *17*, 37–43.

Kramer, J.A., Sagartz, J.E., Morris, D.L. (2007). The application of discovery toxicology and pathology towards the design of safer pharmaceutical lead candidates. *Nat. Rev. Drug Discov.*, *6*, 636–649.

12 Krishnan, S., Hvastkovs, E.G., Bajrami, B., Choudhary, D., Schenkman, J.B., Rusling, J.F. (••). ••. in preparation.

Krishnan, S., Hvastkovs, E.G., Bajrami, B., Jansson, I., Schenkman, J.B., Rusling, J.F. (2007). Genotoxicity screening for N-nitroso compounds. Electrochemical and electrochemiluminescent detection of human enzyme-generated DNA damage from N-nitrosopyrrolidine. *Chem. Commun.*, 1713–1715.

Kuang, L., Biran, I., Walt, D. (2004). Living bacterial cell array for genotoxin monitoring. *Anal. Chem.*, *76*, 2902–2909.

Kupfer, R., Liu, S.Y., Allentoff, A.J., Thompson, J.A. (2001). ••. *Biochemistry*, *40*, 11490–11501.

Lee, J., Mitchell, R., Kim, B., Cullen, D., Gu, M. (2005a). A cell array biosensor for environmental toxicity analysis. *Biosens. Bioelectron.*, *21*, 500–507.

Lee, M., Park, C., Dordick, J., Clark, D. (2005b). Metabolizing enzyme toxicology assay chip (MetaChip) for high throughput microscale toxicity analyses. *Proc. Natl. Acad. Sci. U.S.A.*, *102*, 983–987.

Leland, J.K., Powell, M.J. (1990). ••. *J. Electrochem. Soc.*, *137*, 3127–3131.

Li, A., Bode, C., Sakai, Y. (2004). A novel in vitro system, the integrated discrete multiple organ cell culture (IdMOC) system, for the evaluation of human drug toxicity: comparative cytotoxicity of tamoxifen towards normal human cells from five major organs and MCF-7 adenocarcinoma breast cells. *Chem. Biol. Interact.*, *150*, 129–136.

Liebler, D.C., Guengerich, F.P. (2005). Elucidating the mechanisms of drug-induced toxicity. *Nat. Rev. Drug Dev.*, *4*, 410–420.

Lindon, J.C., Nicholson, J.K., Holmes, E., Antti, H., Bollard, M.E., Keun, H., Beckonert, O., Ebbels, T.M., Reily, M.D., Robertson, D.R., Stevens, G.J., Luke, P., Breau, A.P., Cantor, G.H., Bible, R.H., Niederhauser, U., Senn, H., Schlotterbeck, G., Sideelmann, U.G., Laursen, S.M., Tymiak, A., Car, B.D., Lehman-McKeeman, L., Colet, J.-M., Loukaci, A., Thomas, C. (2003). Contemporary issues in toxicology: the role of metabonomics in toxicology and its evaluation by the COMET project. *Toxicol. Appl. Pharm.*, *187*, 137–146.

Lippard, S.J., Berg, J.M. (1994). *Principles of Bioorganic Chemistry*, University Science Books, Mill Valley, CA.

Lvov, Y. (2000). *Protein Architecture: Interfacing Molecular Assemblies and Immobilization Biotechnology* (eds Y. Lvov and H. Möhwald), Marcel Dekker, New York, pp. 125–167.

Lvov, Y. (2001). *Handbook of Surfaces and Interfaces of Materials*, Vol. *3*. Nanostructured Materials, Micelles and Colloids (ed. R.W. Nalwa), Academic Press, San Diego, pp. 170–189.

Lvov, Y., Caruso, F. (2001). ••. *Anal. Chem.*, *73*, 4212–4217.

McNeish, J. (2004). Embryonic stem cells in drug discovery. *Nat. Rev. Drug Dev.*, *3*, 70–80.

Marnett, L.J., Burcham, P.C. (1993). Endogenous DNA adducts: potential and paradox. *Chem. Res. Toxicol.*, *6*, 771–785.

Mayne, J.T., Ku, W.W., Kennedy, S.P. (2006). Informed toxicity assessment in drug discovery: systems-based toxicology. *Curr. Opin. Drug Discov. Devel.*, *9*, 75–83.

Mitchell, R., Gu, M. (2004a). An Escherichia coli biosensor capable of detecting both genotoxic and oxidative damage. *Appl. Microbiol. Biotechnol.*, *64*, 46–52.

Mitchell, R., Gu, M. (2004b). Construction and characterization of novel dual stress-responsive bacterial biosensors. *Biosens. Bioelectron.*, *19*, 977–985.

Montrescu, E.R., Otto, A.M., Brischwein, M., Zahler, S., Wolf, B. (2005). Dynamic analysis of metabolite effects of chloroacetaldehyde and cytochalasin B on tumor cells using bioelectronic sensor chips. *J. Cancer Res. Clin. Oncol.*, *131*, 683–691.

Mortishire-Smith, R.J., Skiles, G.L., Lawrence, J.W., Spence, S., Nicholls, A.W., Johnson, B.A., Nicholson, J.K. (2004). Use of metabonomics to identify impaired fatty acid metabolism as the mechanism of drug induced toxicity. *Chem. Res. Toxicol.*, *17*, 165–173.

Mugweru, A., Rusling, J.F. (2006). Studies of DNA damage inhibition by dietary antioxidants using metallopolyion/DNA sensors. *Electroanalysis*, *18*, 327–332.

Mugweru, A., Yang, J., Rusling, J.F. (2004). Comparison of hemoglobin and myoglobin for in-situ metabolite generation in chemical toxicity sensors using a metallopolymer catalyst for DNA damage detection. *Electroanalysis*, *16*, 1132–1138.

Munge, B., Estavillo, C., Schenkman, J.B., Rusling, J.F. (2003). Optimizing electrochemical and peroxide-driven oxidation of styrene with ultrathin polyion films containing cytochrome P450cam and myoglobin. *Chembiochem*, *4*, 82–89.

Nasser, A.E.F., Kamel, A.M., Clarimont, C. (2004). Improving the decision making process in structural modification of drug candidates: reducing toxicity. *Drug Discov. Today*, *9*, 1055–1064.

Natarajan, A., Molnar, P., Sieverdes, K., Jamshidi, A., Hickman, J. (2006). Microelectrode array readings of cardiac action potentials as a high throughput method to evaluate pesticide toxicity. *Toxicol. In Vitro*, *20*, 375–381.

Neilson, A.H. (ed.) (1998). *PAHs and Related Compounds*, Springer, Berlin.

Newton, R.K., Aardema, M., Aubrecht, J. (2004). The utility of DNA microarrays for characterizing genotoxicity. *Environ. Health Pers.*, *112*, 420–422.

Nicholson, J.K., Connelly, J., Lindon, J.C., Holmes, E. (2002). Metabonomics: a platform for studying drug toxicity and gene function. *Nat. Rev. Drug Discov.*, *1*, 156–161.

O'Brien, P., Irwin, W., Diaz, D., Cofield, H., Krejsa, C., Slaughter, M., Gao, B., Kaludercic, N., Angeline, A., Bernardi, P., Brain, P., Hougham, C. (2006). High concordance of drug-induced human hepatotoxicity with in vitro cytotoxicity measured in a novel cell based model using high content screening. *Arch. Toxicol.*, *80*, 580–604.

Oda, Y., Nakamura, S., Oki, I., Kato, T., Shinagawa, H. (1985). Evaluation of a new system (umu-test) for the detection of environmental mutagens and carcinogens. *Mutat. Res.*, *147*, 212–229.

Ortiz de Montellano, P.R. (2005). *Cytochrome P-450: Structure, Mechanism, and Biochemistry*, 3rd edn, Kluwer Academic/Plenum, New York.

Ortiz de Montellano, P.R., De Voss, J.J. (2002). ••. *Nat. Prod. Rep.*, *19*, 477–493.

Owens, J. (2005). Do microarrays match up? *Nat. Rev. Drug Discov.*, *4*, 459.

Park, K., Williams, D.P., Naisbitt, D.J., Kitteringham, N.R., Pirmohamed, M. (2005). Investigation of toxic metabolites during drug development. *Toxicol. Appl. Pharmacol.*, *207*, S425–S434.

Pauwels, W., Vodiceka, P., Servi, M., Plna, K., Veulemans, H., Hemminki, K. (1996). ••. *Carcinogenisis*, *17*, 2673–2680.

Phillips, D.H., Farmer, P.B., Beland, F.A., Nath, R.G., Poirier, M.C., Reddy, M.V., Turtletaub, K.W. (2000). ••. *Environ. Mol. Mutagen.*, *35*, 222–233.

Preussmann, R., Stewart, B.W. (1984). N-Nitroso carcinogens, in *Chemical Carcinogenesis* (ed. C.E. Searle), ACS monograph 182, American Chemical Society, Washington, DC, pp. 643–828.

Rahimtula, A.D., O'Brien, P.J., Seifried, H.E., Jerina, D.M. (1978). The mechanism of action of cytochrome P-450. Occurrence of the "NIH shift" during hydroperoxide-dependent aromatic hydroxylations. *Eur. J. Biochem.*, *89*, 133–141.

Riley, M.R., Lucas, P., Le Coq, D., Juncker, C., Boesewetter, D.E., Collier, J.L., DeRosa, D.M., Katterman, M.E., Boussard-Pledel, C., Bureau, B. (2006). Lung cell fiber evanescent wave spectroscopic biosensing of inhalation health hazards. *Biotechnol. Bioeng.*, *95*, 599–612.

Rogan, E.G., Devanesan, P.D., Ramakrishna, N.V.S., Higgenbotham, S., Padvavathi, N.S., Chapman, K., Cavalieri, E.L., Jeong, H., Jankowiak, R., Small, G.J. (1993). ••. *Chem. Res. Toxicol.*, *6*, 356–363.

Rubinstein, I., Bard, A.J. (1980). ••. *J. Am. Chem. Soc.*, *102*, 6642–6644.

Rusling, J.F. (2004). ••. *Biosens. Bioelectron.*, *20*, 1022–1028.

Rusling, J.F. (2005). *Electrochemistry of Nucleic Acids and Proteins* (eds E. Palecek, F. Scheller and J. Wang), Elsevier, pp. 433–450.

Rusling, J.F., Hvastkovs, E.G., Hull, D.O., Schenkman, J.B. (2007). Biochemical applications of ultrathin films of enzymes, polyions and DNA (feature article). *Chem. Commun.*, DOI: 10.1039/b709121b.

Rusling, J.F., Hvastkovs, E.G., Schenkman, J.B. (2007). ••. *Curr. Opin. Drug Discov. Devel.*, *10*, 67–73.

Sasaki, Y.F., Sekihashi, K., Izumiyama, F., Nishidate, E., Saga, A., Ishida, K., Truda, S. (2000). The Comet assay with multiple mouse organs: comparison of Comet assay results and carcinogenicity with 208 chemicals selected from the IARC monographs and U.S. NTP Carcinogenicity Database. *Crit. Rev. Toxicol.*, *30*, 629–799.

Scharer, O.D. (2003). ••. *Angew. Chem. Int. Ed. Engl.*, *42*, 2946–2974.

Schenkman, J.B., Greim, H. (eds) (1993). *Cytochrome P450*, Springer-Verlag, Berlin.

Schwartz, M.P., Derfus, A.M., Alvarez, S.D., Bhatia, S.N., Sailor, M.J. (2006). The smart petri dish: a nanostructured photonic crystal for real-time monitoring of living cells. *Langmuir*, *22*, 7084–7090.

Schweitzer, B., Wiltshire, S., Lambert, J., O'Malley, S., Kukanskis, K., Zhu, Z., Kingsmore, S.F., Lizardi, P.M., Ward, D.C. (2000). Immunoassays with rolling circle DNA amplification: a versatile platform for ultrasensitive antigen determination. *Proc. Natl. Acad. Sci. U.S.A.*, *97*, 10113–10119.

Shuga, J., Zhang, J., Samson, L.D., Lodish, H.F., Griffith, L.G. (2007). In vitro erythropoiesis from bone marrow-derived progenitors provides a physiological assay for toxic and mutagenic compounds. *Proc. Natl. Acad. Sci. U.S.A.*, *104*, 8737–8742.

Shutava, T., Zheng, Z., John, V., Lvov, Y. (2004). ••. *Biomacromolecules*, *5*, 914–921.

Singh, N.P., McCoy, M.T., Tice, R.R., Schneider, E.L. (1998). A simple technique for quantitation of low levels of DNA damage in individual cells. *Exp. Cell. Res.*, *175*, 184–191.

So, M., Hvastkovs, E.G., Schenkman, J.B., Rusling, J.F. (2007). Electrochemiluminescent/voltammetric toxicity screening sensor using enzyme-generated DNA damage. *Biosens. Bioelectron.*, *23* (4), 492–498.

13

Solomun, T., Sturm, H. (2007). Bringing electrons and microarray technology together. *J. Phys. Chem. B*, *111*, 10636–10638.

Sreekumar, A., Nyati, M.K., Varambally, S., Barrette, T.R., Ghosh, D., Lawrence, T.S., Chinnaiyan, A.M. (2001). Profiling of cancer cells using protein microarrays: discovery of novel radiation-regulated proteins. *Cancer Res.*, *61*, 7585–7593.

Stoll, D., Bachmann, J., Templin, M.F., Joos, T.O. (2004). Microarray technology: an increasing variety of screening tools for proteomic research. *Drug Discov. Today: Targets*, *3*, 24–31.

Styles, J.A., Clark, H., Festing, M.F.W., Rew, D.A. (2001). Automation of mouse micronucleus genotoxicity assay by laser scanning cytometry. *Cytometry*, *44*, 153–155.

Tanaka, E., Terada, M., Misawa, S. (2000). ••. *J. Clin. Pharm. Ther.*, *3*, 165–175.

Tarun, M., Rusling, J.F. (2005a). Measuring DNA nucleobase adducts using neutral hydrolysis and liquid chromatography-mass spectrometry. *Crit. Rev. Eukaryot. Gene Expr.*, *15*, 295–315.

Tarun, M., Rusling, J.F. (2005b). Quantitative measurement of DNA adducts using neutral hydrolysis and LC-MS. Validation of genotoxicity sensors. *Anal. Chem.*, *77*, 2056–2062.

Tarun, M., Rusling, J.F. (2006). Genotoxicity screening using biocatalyst-DNA films and capillary LC-MS/MS. *Anal. Chem.*, *78*, 624–627.

Todorovic, R., Ariese, F., Devenesan, P., Jankowiak, R., Small, G.J., Rogan, E.G., Cavalieri, E.L. (1997). ••. *Chem. Res. Toxicol.*, *10*, 941–947.

Ulrich, R., Friend, S.H. (2002). Toxicogenomics and drug discovery: will new technologies help us produce better drugs. *Nat. Rev. Drug Discov.*, *1*, 84–88.

Umemoto, A., Komaki, K., Monden, Y., Suwa, M., Kanno, Y., Kitagawa, M., Suzuki, M., Lin, C.-X., Ueyama, Y., Momen, M.A., Ravindernath, A., Shibutani, S. (2001). ••. *Chem. Res. Toxicol.*, *14*, 1006–1013.

Van Gompel, J., Woestenborghs, F., Beerens, D., Mackie, C., Cahill, P.A., Knight, A.W., Billinton, N., Tweats, D.J., Walmsley, R.M. (2005). An assessment of the utility of the yeast GreenScreen assay in pharmaceutical screening. *Mutagenesis*, *20*, 449–454.

Vanhoutte, K., Dongen, W., Hoes, I., Lemiere, F., Esmans, E.L., Van Onckelen, H., Van den Eckhout, E., Soest, R.E.J., Hudson, A.J. (1997). Development of a nanoscale liquid chromatography/electrospray mass spectrometry methodology for the detection and quantification of DNA adducts. *Anal. Chem.*, *69*, 3161–3168.

Vansant, G., Pezzoli, P., Saiz, R., Birch, A., Duffy, C., Ferre, F., Monforte, J. (2006). Gene expression analysis of troglitazone reveals its impact on multiple pathways in cell culture: a case for in vitro platforms combined with gene expression analysis for early (idiosyncratic) toxicity screening. *Int. J. Toxicol.*, *25*, 85–94.

Vignati, L., Turlizzi, E., Monaci, S., de Grossi, P., Kanter, P., Monshouwe, M. (2005). An in vitro approach to detect metabolite toxicity due to CYP3A4-dependent bioactivation of xenobiotics. *Toxicology*, *216*, 154–167.

Viravaidya, K., Sin, A., Shuler, M. (2004). Development of a microscale cell culture analog to probe naphthalene toxicity. *Biotechnol. Prog.*, *20*, 316–323.

Wang, B., Jansson, I., Schenkman, J.B., Rusling, J.F. (2005). Evaluating enzymes that generate genotoxic benzo[a]pyrene metabolites using sensor arrays. *Anal. Chem.*, *77*, 1361–1367.

Wang, M., Cheng, G., Sturla, S.J., Shi, Y., McIntee, E.J., Villalta, P.W., Upadhyaya, P., Hecht, S.S. (2003). ••. *Chem. Res. Toxicol.*, *16*, 616–626.

Wang, M., McIntee, E.J., Shi, Y., Cheng, G., Upadhyaya, P., Villalta, P.W., Hecht, S.S. (2001). ••. *Chem. Res. Toxicol.*, *14*, 1435–1445.

Warren, A.J., Shields, P.G. (1997). ••. *Proc. Soc. Exp. Biol. Med.*, *216*, 172–180.

Werringloer, J., Kawano, S., Estabrook, R.W. (1980). Comparison of the interaction of cumene hydroperoxide and hydrogen peroxide with liver microsomal cytochromes, in *Microsomes, Drug Oxidations, and Chemical Carcinogenesis* (eds M.C. Coon, A.H. Conney, R.W. Estabrook and H.V. Gelboin), Academic Press, New York, pp. 403–406.

White, R.E., Sligar, S.G., Coon, M.W. (1980). Evidence for a homolytic mechanism of peroxide oxygen-oxygen bond cleavage during substrate hydroxylation by cytochrome P-450. *J. Biol. Chem.*, *255*, 11108–11111.

Xiao, C., Luong, H.T. (2005). Assessment of cytotoxicity by emerging impedance spectroscopy. *Toxicol. Appl. Pharm.*, *206*, 102–112.

Xing, J.Z., Zhu, L., Jackson, J., Gabos, S., Sun, X.-J., Wang, X.-b., Xu, X. (2005). Dynamic monitoring of cytotoxicity on microelectrode sensors. *Chem. Res. Toxicol.*, *18*, 154–161.

Xu, X.-H., Bard, A.J. (1995). ••. *J. Am. Chem. Soc.*, *117*, 2627–2631.

Xu, X.-H., Yang, H.C., Mallouk, T.E., Bard, A.J. (1994). ••. *J. Am. Chem. Soc.*, *116*, 8386–8387.

Yang, J., Wang, B., Rusling, J.F. (2005). Genotoxicity sensor response correlated with DNA nucleobase damage rates. *Mol. Biosyst.*, *1*, 251–259.

Young-Scaime, R., Wang, M., Chung, F.-L., Hecht, S.S. (1995). ••. *Chem. Res. Toxicol.*, *8*, 607–616.

Zamenhof, S., Arikawa, S. (1966). Depurination and alkylation of DNAs of different base compositions. *Mol. Pharmacol.*, *2*, 570–573.

Zhang, X., Chen, H., Zhang, H. (2007). ••. *Chem. Commun.*, 1395–1405.

Zhang, X., Wang, W., Yu, W., Xie, Y., Zhang, X., Zhang, Y., Ma, X. (2005). Development of an in vitro multicellular tumor spheroid model using microencapsulation and its application in anticancer drug screening and testing. *Biotechnol. Prog.*, *21*, 1289–1296.

Zhou, L., Yang, J., Estavillo, C., Stuart, J.D., Schenkman, J.B., Rusling, J.F. (2003). Toxicity screening by electrochemical detection of DNA damage by metabolites generated *in-situ* in ultrathin DNA-enzyme films. *J. Am. Chem. Soc.*, *125*, 1431–1436.

Zhu, J., Wang, X., Yu, W., Abassi, Y.A. (2006). Dynamic and label-free monitoring of natural killer cell cytotoxic activity using electronic cell sensor arrays. *J. Immunol. Methods*, *309*, 25–33.

Zoltewicz, J.A., Clark, D.F. (1972). Kinetics and mechanism of the hydrolysis of guanosine and 7-methylguanosine nucleosides in perchloric acid. *J. Org. Chem.*, *37*, 1193–1197.

Author Queries

Dear Author,

During the preparation of your manuscript for publication, the questions listed below have arisen. Please attend to these matters and return this form with your proof.

Many thanks for your assitstance.

Query	Query	Remarks
Figure	Note that figures may have been relabelled for readability, please check.	
1	Au: Is the short title OK? If not, please provide one.	
2	Au: Please confirm the citations are correct.	
3	Au: Should SCE be written in full? If so, please provide the full form.	
4	Au: Please confirm the citations are correct.	
5	Au: (Bajrami et al., submitted) Please provide the year of publication.	
6	Au: Should GC be written in full? If so, please provide the full form.	
7	Au: Should SRM be written in full? If so, please provide the full form.	
8	Au: (Krishnan *et al.*, in preparation) Please provide the year of publication.	
9	Au: The letters **a** and **b** have been added to distinguish reference citations with the same author group and year of publication.	
10	Au: Please provide the article title of all the journal reference entries.	

11	Au: (Bajrami et al. submitted) Has this work been accepted for publication? If yes, please update the year of publication, volume number and page range; if not, please remove it from the list and cite it as unpublished reference in the text, i.e. '**Bajrami et al., unpublished**'.	
12	Au: (Krishnan et al. in preparation) Has this work been accepted for publication? If yes, please update the year of publication, volume number and page range; if not, please remove it from the list and cite it as unpublished reference in the text, i.e. '**Krishnan et al., unpublished**'.	
13	Au: (So et al. 2007) The missing volume number and page range have been added. Please confirm this is correct.	
14	Au: (Fig. 13.4) Please provide the definition for $I_{p,f}/I_{p,i}$.	
15	Au: (Fig. 13.12) Please provide the year of publication for Bajrami et al.	
16	Au: (Fig. 13.13) Please provide the year of publication for Bajrami et al.	
17	Au: Please provide the caption for Scheme 13.2.	
18	Au: Please provide the caption for Scheme 13.3.	
19	Au: (Scheme 13.6) Should A and B be given a description?	